



# Metal-Organic Frameworks in Polymer Science: Polymerization Catalysis, Polymerization Environment, and Hybrid Materials

Bernhard V. K. J. Schmidt

The development of metal-organic frameworks (MOFs) has had a significant impact on various fields of chemistry and materials science. Naturally, polymer science also exploited this novel type of material for various purposes, which is due to the defined porosity, high surface area, and catalytic activity of MOFs. The present review covers various topics of MOF/polymer research beginning with MOF-based polymerization catalysis. Furthermore, polymerization inside MOF pores as well as polymerization of MOF ligands is described, which have a significant effect on polymer structures. Finally, MOF/polymer hybrid and composite materials are highlighted, encompassing a range of material classes, like bulk materials, membranes, and dispersed materials. In the course of the review, various applications of MOF/polymer combinations are discussed (e.g., adsorption, gas separation, drug delivery, catalysis, organic electronics, and stimuli-responsive materials). Finally, past research is concluded and an outlook toward future development is provided.

## 1. Introduction

The combination of polymers with inorganic materials is a common way to achieve new properties and applications or to merge properties.<sup>[1–3]</sup> Hence, features of the inorganic material can be introduced into polymer materials and—at best—a sum of the individual properties or even novel features are obtained, which might lead to a material with unprecedented and advanced properties. As such, improvement for various applications can be targeted as well as new applications accomplished. Since their first introduction, metal-organic


frameworks (MOFs) have attracted significant attention in inorganic chemistry as well as materials science.<sup>[4,5]</sup> In the meantime, MOFs have found their way into all areas of chemical sciences, which is closely related to their well-defined porous structure and modular buildup that allows tailoring according to specific needs. MOFs are crystalline compounds consisting of 3D ordered metal-ligand complexes and a broad variety of ligands and metal ions were studied in the past decades (Table 1).<sup>[6–15]</sup> In contrast to classical coordination chemistry, MOFs are formed from multifunctional ligands that facilitate complex formation in a repetitive manner, which can be designated as a supramolecular polymerization in three dimensions (Scheme 1). The structure of the crystalline MOF correlates directly

with the utilized ligands, that is, their geometry and functionality, and metal ions, that is, the metal ion size, geometry, and association constant. As such, the MOF structure is highly tunable regarding various properties, for example, pore sizes, metal incorporation, or rigidity of the framework. Hence, MOFs have found various applications, for example, in the field of catalysis,<sup>[16]</sup> gas storage,<sup>[17]</sup> or nanomedicine.<sup>[18]</sup>

A combination of MOFs and polymers seems to be a promising choice for a composite/hybrid material as favorable properties of both material classes can be combined that way. MOFs feature well-defined porosity, metal content, and defined crystal structures, while polymers add processability, mechanical/chemical durability, and biomedical applications to the picture. MOFs are of particular interest for applications like gas adsorption or catalysis due to their large surface area, well-defined pore structure, and incorporation of metal ions. In such a way, significant amounts of molecules can be stored.<sup>[20,21]</sup> Moreover, the defined pore sizes allow gas uptake with high selectivity. In that regard a combination with polymers can lead to favorable effects in addition to improved mechanical properties of MOF/polymer composites, for example, increased gas permeation selectivity or adsorption capacity. Additionally, the incorporation of metal ions endows MOFs with catalytic properties.<sup>[22]</sup> Therefore, MOFs act as heterogeneous catalysts, for example, in the light-induced copper catalyzed azide alkyne cycloaddition (CuAAC) reaction or the cycloaddition of CO<sub>2</sub> and epoxides.<sup>[23,24]</sup> Furthermore, MOFs can be utilized as heterogeneous polymerization catalyst for metal catalyzed polymerization reactions,

Dr. B. V. K. J. Schmidt  
Max Planck Institute of Colloids and Interfaces  
Am Mühlenberg 1, 14476 Potsdam, Germany  
E-mail: bernhard.schmidt@mpikg.mpg.de;  
bernhard.schmidt@glasgow.ac.uk

Dr. B. V. K. J. Schmidt  
School of Chemistry  
University of Glasgow  
Joseph Black Building, Glasgow G12 8QQ, UK

 The ORCID identification number(s) for the author(s) of this article can be found under <https://doi.org/10.1002/marc.201900333>.

© 2019 The Authors. Published by WILEY-VCH Verlag GmbH & Co. KGaA, Weinheim. This is an open access article under the terms of the Creative Commons Attribution-NonCommercial License, which permits use, distribution and reproduction in any medium, provided the original work is properly cited and is not used for commercial purposes.

DOI: 10.1002/marc.201900333

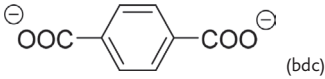
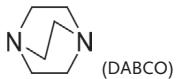
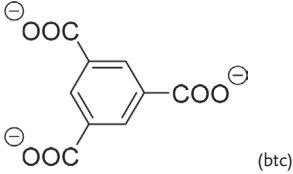
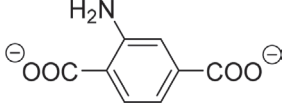
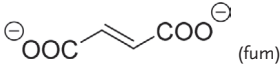
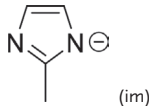
for example, atom transfer radical polymerization (ATRP) or coordination polymerization.<sup>[25,26]</sup> Another important point in MOF-mediated chemical reactions is the effect of porosity or the confined environment on product formation. As the MOF pores are rather small with diameters in the nanometer range, educt trajectories inside are well defined and pore walls can favor specific product geometries. Hence, product selectivity can be directed and tailored as shown by Yaghi and coworkers for the gas phase conversion of methylcyclopentane.<sup>[27]</sup> As such, enhanced control over the regio- and stereochemistry of chemical reactions features an interesting aspect to polymerizations as well, namely tacticity control.<sup>[28,29]</sup> MOFs can be further used as templates for polymers with unprecedented pore structures<sup>[30]</sup> or in combination with polymers to obtain porous dispersed particles/capsules.<sup>[31]</sup>

In the following review, a broad overview of the research area that combines MOFs and polymers is presented. MOFs as polymerization catalysts for reversible deactivation radical polymerization (RDRP), photopolymerization, and coordination polymerization will be addressed. Moreover, the review summarizes the efforts regarding polymerization in MOF pores,

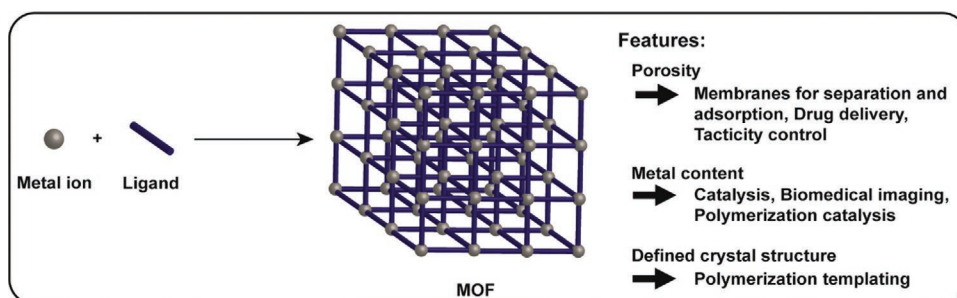


**Bernhard V. K. J. Schmidt** completed his Ph.D. in 2013 with Prof. Barner-Kowollik at the Karlsruhe Institute of Technology and subsequently a postdoc with Prof. Hawker at the University of California, Santa Barbara. Afterward, he joined the department of Prof. Antonietti at the Max Planck Institute of Colloids and Interfaces as a group leader and was awarded with the Dr. Hermann Schnell Fellowship 2018. Recently, he joined the University of Glasgow as a lecturer in synthetic polymer chemistry. His research focuses on block copolymer self-assembly, metal-organic framework/polymer hybrids, and carbon nitride/polymer hybrid materials.

**Table 1.** Common MOFs and their components.

Formula	Abbreviation	Metal ion	Ligands	Reference
$M_2(\text{bdc})_2(\text{DABCO})$	–	$\text{Cu}^{2+}, \text{Zn}^{2+}$	 (bdc)  (DABCO)	[6,19]
$\text{Cu}_3(\text{btc})_2$	HKUST-1	$\text{Cu}^{2+}$	 (btc)	[7]
$\text{Zn}_4\text{O}(\text{bdcNH}_2)_3$	IRMOF-3	$\text{Zn}^{2+}$		[8]
$\text{M}(\text{bdc})(\text{OH})$	MIL-53	$\text{Al}^{3+}, \text{Sc}^{3+}, \text{Fe}^{3+}$	bdc	[9]
$\text{V}(\text{OH})(\text{bdc})$	MIL-68	$\text{V}^{3+}$	bdc	[10]
$\text{MO}(\text{H}_2\text{O})_2\text{X}(\text{fum})_3$	MIL-88a	$\text{Fe}^{3+}, \text{Cr}^{3+}$	 (fum)	[11]
$\text{M}_3\text{O}(\text{OH})(\text{H}_2\text{O})_2(\text{bdc})_3$	MIL-101	$\text{Fe}^{3+}, \text{Cr}^{3+}$	bdc	[12]
$\text{Zn}_4\text{O}(\text{bdc})_3$	MOF-5 = IRMOF-1	$\text{Zn}^{2+}$	bdc	[13]
$\text{Zr}_6\text{O}_4(\text{OH})_4(\text{bdc})_6$	UiO-66	$\text{Zr}^{4+}$	bdc	[14]
$\text{Zn}(\text{im})_2$	ZIF-8	$\text{Zn}^{2+}$	 (im)	[15]

HKUST, Hong Kong University of Science and Technology; IRMOF, Isorecticular metal-organic framework; MIL, Materials Institute Lavoisier; UiO, Universitet i Oslo; X, F, Cl, acetate; ZIF, Zeolitic imidazolate framework.



**Scheme 1.** Formation of an MOF via ligand and metal ion complexation as well as an overview of MOF features with respect to polymer science.

highlighting radical polymerization approaches as well as other polymerization mechanisms. In addition, polymerization of MOF ligands and the formation of MOFs via polymeric ligands are presented as well. Finally, MOF/polymer hybrid materials will be displayed with topics ranging from bulk material composites, MOF/polymer membranes, to dispersed MOF/polymer hybrids.

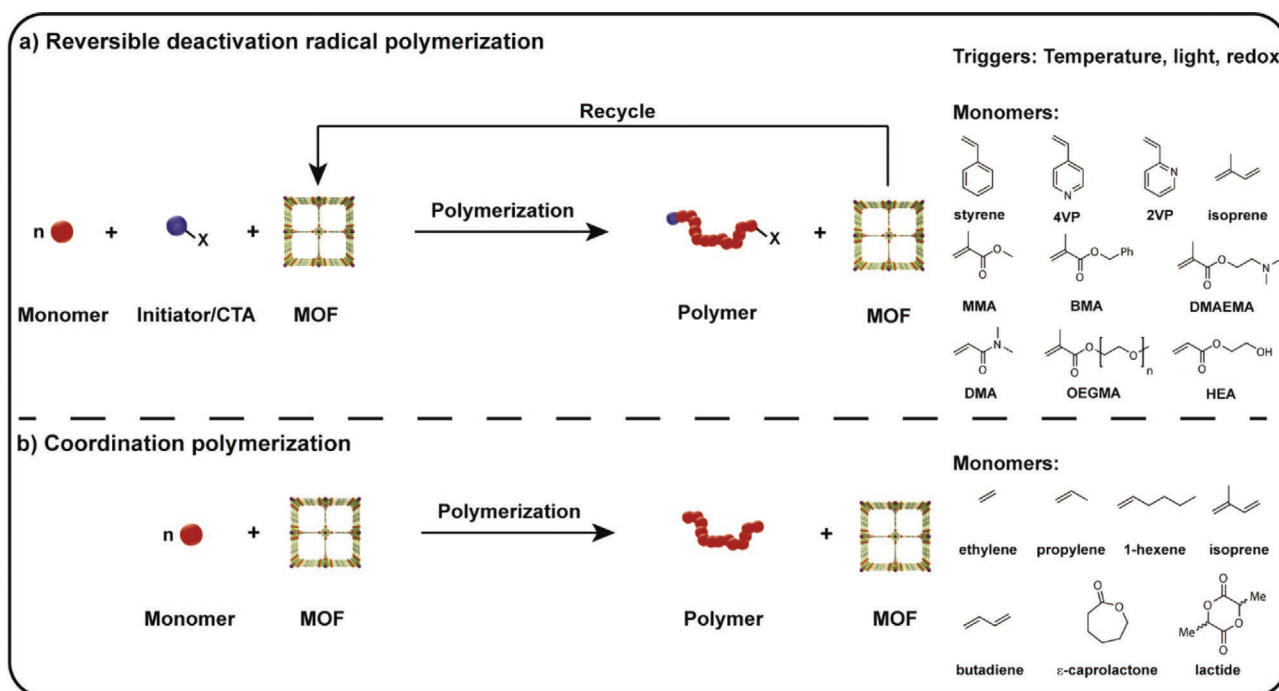
## 2. MOF-Based Polymerization Catalysts

Utilization of MOFs as heterogeneous polymerization catalysts has proven to be a useful approach for the synthesis of polymers (Scheme 2).<sup>[32]</sup> In the area of RDRP, decent control over the polymerization reaction was observed as well as significant reaction rates, especially in the case of photopolymerization. In addition, the features of recyclability and reduced metal contamination in the product are definitive adding value, which is mainly due to the heterogeneous nature of MOF catalysts. A field

in polymer science that is based on monomer metal interactions is coordination polymerization. As such, MOFs are promising catalysts in coordination polymerization as well. Nevertheless, a MOF polymerization catalyst will always introduce metal into the system that might be unwanted for several applications especially in the biomedical field. Moreover, the utilization of MOFs requires a more complex catalyst compared to small molecules and thus an increased synthetic effort prior to polymerization. Overall, the approach of MOFs as polymerization catalysts is a true alternative for preparative polymer chemistry. Even though some disadvantages are present, MOF polymerization catalysis offers a broad range of new opportunities for polymer chemists.

### 2.1. Reversible Deactivation Radical Polymerization

One of the major RDRP methods is based on metal catalysts, that is, ATRP.<sup>[33,34]</sup> Therefore, it is obvious to use MOFs as



**Scheme 2.** Overview of MOF catalyzed polymerization and respective scope of monomers: a) reversible deactivation radical polymerization and b) coordination polymerization (4VP, 4-vinylpyridine; 2VP, 2-vinylpyridine; MMA, methyl methacrylate; BMA, benzyl methacrylate; DMAEMA, dimethylaminoethyl methacrylate; DMA, *N,N*-dimethylacrylamide; OEGMA, oligo(ethyleneglycol) methacrylate; HEA, 2-hydroxyethyl acrylate).

catalysts for such polymerization reactions via substitution of small metal complexes with MOFs. As ATRP is usually Cu or Fe mediated,<sup>[34]</sup> utilization of Cu- or Fe-based MOFs seems to be an appropriate choice for MOF-based polymerization catalysis. Our team showed a way to activate [Cu<sub>2</sub>bdc<sub>2</sub>DABCO] (bdc, benzene dicarboxylate; DABCO, diaminobicyclooctane) thermally based on amine compounds, for example, additionally added DABCO.<sup>[35]</sup> To perform polymerizations, initiator, monomer, Cu(II) MOF, and DABCO were mixed and heated to start the polymerization in a heterogeneously catalyzed process. The Cu(II) was reduced in situ to form catalytically active Cu(I). Hence, an activators regenerated by electron transfer (ARGET) ATRP was performed.<sup>[36]</sup> The process was performed with ethyl  $\alpha$ -bromoisobutyrate (EBiB) as initiator as well as various monomers, that is, styrene, benzyl methacrylate (BMA), 4-vinyl pyridine (4VP), or isoprene. The polymerizations revealed a controlled process as observed via polymerization kinetics, narrow molar mass distributions, and block copolymer synthesis. It should be noted though that the polymerization process was less controlled in the case of 4VP and isoprene. Nevertheless, 4VP and isoprene are well known for their challenging polymerization behavior in ATRP, for example, due to the side reactions with the catalyst.<sup>[37,38]</sup> Probably the complicated monomers 4VP and isoprene could be polymerized at all, because the MOF Cu catalyst is endowed with superior stability compared to soluble catalyst, which reduces side reactions. Moreover, the polymerization catalysts were recovered easily via solvent addition and centrifugation as well as recycled several times for further polymerization reactions. Notably, the poly(styrene) (PS) products contained

tenfold less amount of Cu contamination compared to conventional ATRP methodologies. Tang and coworkers embedded an iron porphyrin in a zeolitic imidazolate framework-8 (ZIF-8) via a biomimetic mineralization approach that could be used as ATRP catalyst.<sup>[39]</sup> Ascorbic acid was utilized as reducing agent and 2-bromopropionitrile as initiator for the polymerization of oligo(ethylene glycol) methacrylate (OEGMA). Molar masses up to 46 kg mol<sup>-1</sup> were obtained with molecular dispersities ( $\bar{D}$ ) between 1.1 and 1.3. Finally, the catalysts could be removed easily from the reaction mixture and recycled. In another study, Nguyen and coworkers introduced a Fe<sup>3+</sup>-based MOF as catalyst for RDRP activation with microwave irradiation.<sup>[40]</sup> The catalyst was based on Fe<sub>3</sub>O(-CO<sub>2</sub>)<sub>6</sub> secondary building units that acted as Lewis acid in the ATRP of methyl methacrylate (MMA). Recently, Qiao and coworkers described the MOF catalyzed reversible addition-fragmentation chain transfer (RAFT) polymerization.<sup>[41]</sup> Therefore, MOF particles based on Fe(II) and 3,5-pyridine dicarboxylate were activated with glycine and combined with hydrogen peroxide to undergo a Fenton reaction leading to Fe<sup>3+</sup>, a hydroxylate ion, and a hydroxyl radical. The hydroxyl radical acted further as initiator for the RAFT polymerization via trithiocarbonate chain transfer agents at ambient temperature. In such a way, *N,N*-dimethylacrylamide (DMA) and 2-hydroxyethylacrylate (HEA) were polymerized in the presence of air. Moreover, the MOF catalysts could be removed easily and reused after the polymerization. In a similar way, the same team utilized an iron(III)-based MOF, that is, Materials Institute Lavoisier-53 (MIL-53), together with glucose oxidase for the radical formation to initiate RAFT polymerizations (Figure 1).<sup>[42]</sup>

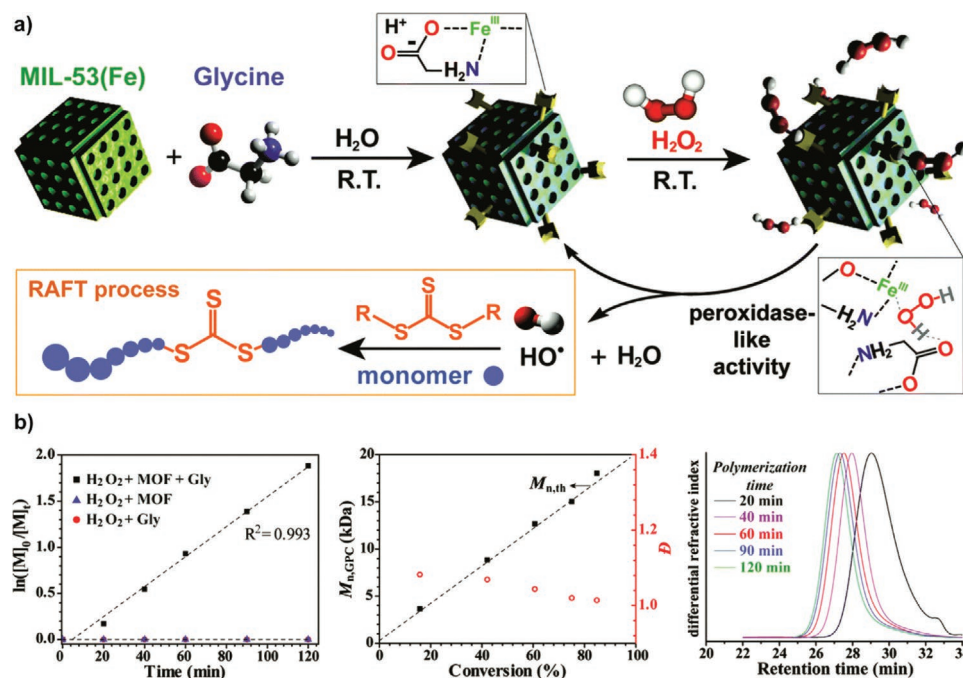


**Figure 1.** MIL-53(Fe) and glycine catalyzed RAFT polymerization: a) Procedure for catalyst preparation and polymerization mechanism. b) Characterization of synthesized PDMA via MOF-facilitated RAFT polymerization (kinetic study, number-average molar mass ( $M_n$ ) and molecular dispersity ( $\bar{D}$ ) data, and size exclusion chromatography (SEC) evaluation). Reproduced with permission.<sup>[42]</sup> Copyright 2019, Royal Society of Chemistry.



## 2.2. Light-Mediated Polymerization

In recent years, light-mediated RDRP has been a major area of research, which is due to convenient features like triggered polymerization, spatial control, and ease of application.<sup>[43–46]</sup> Interestingly, various MOF-based polymerizations can be triggered via light as well. The group of Xing focused on visible-light-induced polymerization. For example, an MOF based on Zn(II), bdc, and anthracene-bipyridine pillar ligands was utilized as photocatalyst to reduce Cu(II) upon visible light irradiation.<sup>[47]</sup> The formed Cu(I) catalyzed the polymerization of MMA in an ATRP fashion via EBiB initiation with molar masses up to 25 kg mol<sup>-1</sup> and  $\bar{D}$  around 1.2. A linear increase of molar mass with conversion was observed as well as the possibility to turn the polymerization on or off. Later on, the monomer scope was extended toward iso-butyl methacrylate, *n*-butyl methacrylate, and styrene as well as another MOF based on Zr(IV) oxo clusters.<sup>[48,49]</sup> Our group described visible-light-mediated polymerizations via a Cu(II) MOF.<sup>[50]</sup> In this case, a straightforward polymerization was observed for 4VP and 2VP, while less activity was observed for *N,N*-dimethylamino ethyl methacrylate (DMAEMA). Interestingly, significantly fast polymerization rates were observed for 4VP, for example, 85% conversion in 1.5 h. Controlled polymerizations were observed leading to narrow, monomodal molar mass distributions ( $\bar{D}$  = 1.2–1.4), controlled molar mass, and block copolymer formation. For the bulk MMA polymerization, no conversion was noted albeit MMA could be polymerized in a controlled way via addition of 4-ethylpyridine, which additionally allowed conclusions regarding the initiation mechanism. First of all, the monomers 4VP, 2VP, and DMAEMA associated with the MOF, which led to a shift in the absorption band, a strengthened light absorption capability, and an increased polymerization rate. Additionally, the nitrogen containing monomers acted as Cu(II) reduction agent as shown before in the case of DABCO addition. The reductive effect of nitrogen containing monomers was indicated by the successful MMA polymerization after addition of 4-ethylpyridine. In a similar way, Phan and coworkers utilized titanium-based MOFs (MOF-901 and MOF-902) for photopolymerization under visible light (**Figure 2**).<sup>[25,51]</sup>

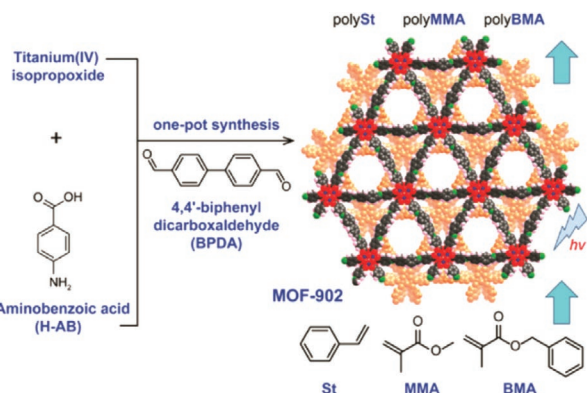


**Figure 2.** Synthesis strategy to produce MOF-901 and MOF-902 based on the in situ Ti-oxo cluster generation and aldehyde functionalities that was used later on for the photopolymerization of methacrylate monomers. Reproduced with permission.<sup>[25]</sup> Copyright 2017, American Chemical Society.

For the polymerization, monomer, that is, MMA, BMA and styrene, ethyl  $\alpha$ -bromophenylacetate as initiator and catalyst were mixed in *N,N*-dimethylformamide (DMF), tetrahydrofuran (THF), or dioxane. The polymerization was performed under visible light irradiation and at first various MOFs were screened regarding their catalytic activity in the polymerization. The best performance was observed in the case of MOF-902, which was ascribed to its favorable light absorption. Overall, molar masses up to 30 kg mol<sup>-1</sup> and  $\bar{D}$  around 1.1–1.2 were obtained. The same method was utilized by Nguyen and coworkers to synthesize a methacrylate-based copolymer employing MMA and a monomer with protected maleimide side groups.<sup>[52]</sup> After polymer synthesis the protecting group was removed and thiol functionalized poly(3-hexylthiophene) grafted onto the backbone to obtain a complex macromolecular architecture. Lalevée and coworkers described the near UV and visible light initiated radical or cationic polymerization of acrylates in laminate or epoxides, respectively.<sup>[14]</sup> As initiator a Fe(III) containing MOF, namely MIL-53, was utilized together with iodonium salt and *N*-vinylcarbazole. The polymerization of 3,4-epoxycyclohexyl-carboxylate was performed under air and conversions of  $\approx$ 60% were obtained in 800 s. In the case of trimethylolpropane triacrylate, radical polymerization was performed that reached 35% conversion after 400 s in the film.

## 2.3. Coordination Polymerization

Coordination polymerization is another polymerization method that relies substantially on metal complexes, albeit on metal-monomer complexes. Thus, MOFs have been utilized as catalysts in coordination polymerization frequently. Especially the defined crystal shape and defined environment of the catalytic center can have a significant impact on the polymerization process and product properties alike, for example, stereoselectivity or molar mass. One of the main monomers polymerized via coordination polymerization in the past is ethylene.<sup>[53]</sup> Regarding the polymerization of ethylene via coordination polymerization, Dincă and coworkers studied a Zn<sub>5</sub>Cl<sub>4</sub>(bis(1H-1,2,3-triazolo[4,5-*b*],[4',5'-*i*])dibenzo[1,4]dioxin)<sub>3</sub> MOF catalyst where some Zn<sup>2+</sup> ions were exchanged with reactive metal centers, namely Ti(III or IV) or Cr(III or II).<sup>[54]</sup> The catalysts produced high molar mass high density polyethylene (PE). Moreover, the morphology of the product could be controlled as the polymer product resembled the MOF crystal shape. The low  $\bar{D}$  of the polymer products suggested single-site catalyst activity. Finally, also copolymers with propylene were obtained. In a similar way, the same group incorporated V(IV) into the MOF structure to obtain another single-site catalyst for ethylene polymerization.<sup>[55]</sup> Notably, propylene was polymerized as well, which led to moderate isotactic polymers (*m* diads around 94%) showing the versatility of MOF catalysts in coordination polymerization. Also Li and coworkers utilized Cr(III)-based MOF for ethylene polymerization.<sup>[56]</sup> Therefore, isorecticular metal-organic framework-3 (IRMOF-3) was modified with salicylideneimine at the surface to associate with Cr(III) ions. The catalysts were activated via methyl aluminumoxane (MAO) or alkylaluminum, while the best activity was observed for triisobutylaluminum yielding high molar

mass PE but broad molar mass distribution. Weckhuysen and coworkers studied Cr-based MIL MOFs for ethylene polymerization with diethyl aluminum chloride cocatalyst.<sup>[57]</sup> The activity of the MOFs was correlated to the stability of the crystallites against fragmentation after cocatalyst addition and MOF porosity. It was assumed that the active species consists of alkylated Cr-complexes, which are much more pronounced in the fragmented and more porous MOF. As such, the effect of the microstructure of the MOF on the polymerization performance was highlighted. Another example regarding ethylene polymerization was described by Lin and coworkers.<sup>[58]</sup> A Zr-benzene tricarboxylate-based MOF was activated with MAO in order to obtain polymerization activity leading to high molar mass PE with low  $\bar{D}$ . Most notably in addition to PE synthesis, MOFs are a route to higher poly(olefins) as well, where polymer tacticity and regiochemistry is playing a major role for product properties. As such coordination polymerization based on MOF catalysts was described by Visseaux and coworkers.<sup>[59]</sup> To that end, Nd MOFs were combined with aluminoxanes for the polymerization of isoprene. The authors found a significant influence of MOF porosity on the polymer product. For example, a higher porosity led to poly(isoprene) with *cis* configuration at low temperatures but *trans* configuration at higher temperatures. For a reason, it was speculated that the monomer arrangement in the pores might change with temperature or the *syn-anti* equilibrium switches. Farha and coworkers polymerized another olefin monomer, namely 1-hexene.<sup>[60]</sup> A Hf-based MOF was employed after introduction of Zr(IV) to produce poly(1-hexene) with high isotacticity and high molar masses up to 680 kg mol<sup>-1</sup>. In another study Dincă tackled coordination polymerization of butadiene (Figure 3).<sup>[61]</sup> Bis(1H-1,2,3-triazolo[4,5-*b*],[4',5'-*i*])dibenzo[1,4]dioxin-based MOFs were utilized, inspired from their earlier work on ethylene polymerization, albeit Co(II) was introduced as metal site. In such a way, poly(1,3-butadiene) with 99% selectivity for the 1,4-*cis* propagation was obtained. In addition, the catalyst was recyclable and low leaching was observed. MOF catalyzed coordination polymerization of a completely different class of monomers was investigated by Wu and coworkers, namely cyclic ester monomers.<sup>[62]</sup> A stable Ti(IV)-butane diol MOF was employed for the polymerization of  $\epsilon$ -caprolactone, L-lactide, and *rac*-lactide at ambient temperature. Hence, poly(esters) with molar masses in the range of 20 kg mol<sup>-1</sup> and  $\bar{D}$  around 1.2–1.4 were obtained.

### 3. MOFs as Polymerization Environment

Not only the polymerization catalyst but also the polymerization environment has a significant effect on the polymerization reaction,<sup>[63]</sup> which is well known from natural systems.<sup>[64,65]</sup> As already mentioned in the Introduction, MOFs provide a well-defined porous network that can be utilized as reaction environment for chemical reactions, that is, to obtain specific regio- or stereoisomers.<sup>[66,67]</sup> Hence, the utilization of MOFs as reaction environment for polymerizations provides confined space affecting orientation of individual monomers inside of the nanochannels.<sup>[68]</sup> Due to the defined pore structure of MOFs, polymerization inside of

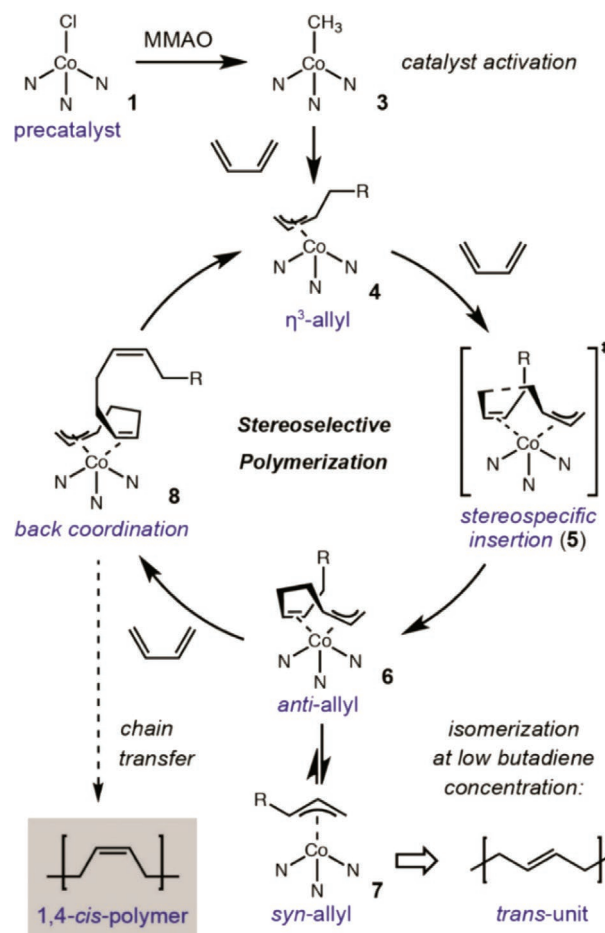
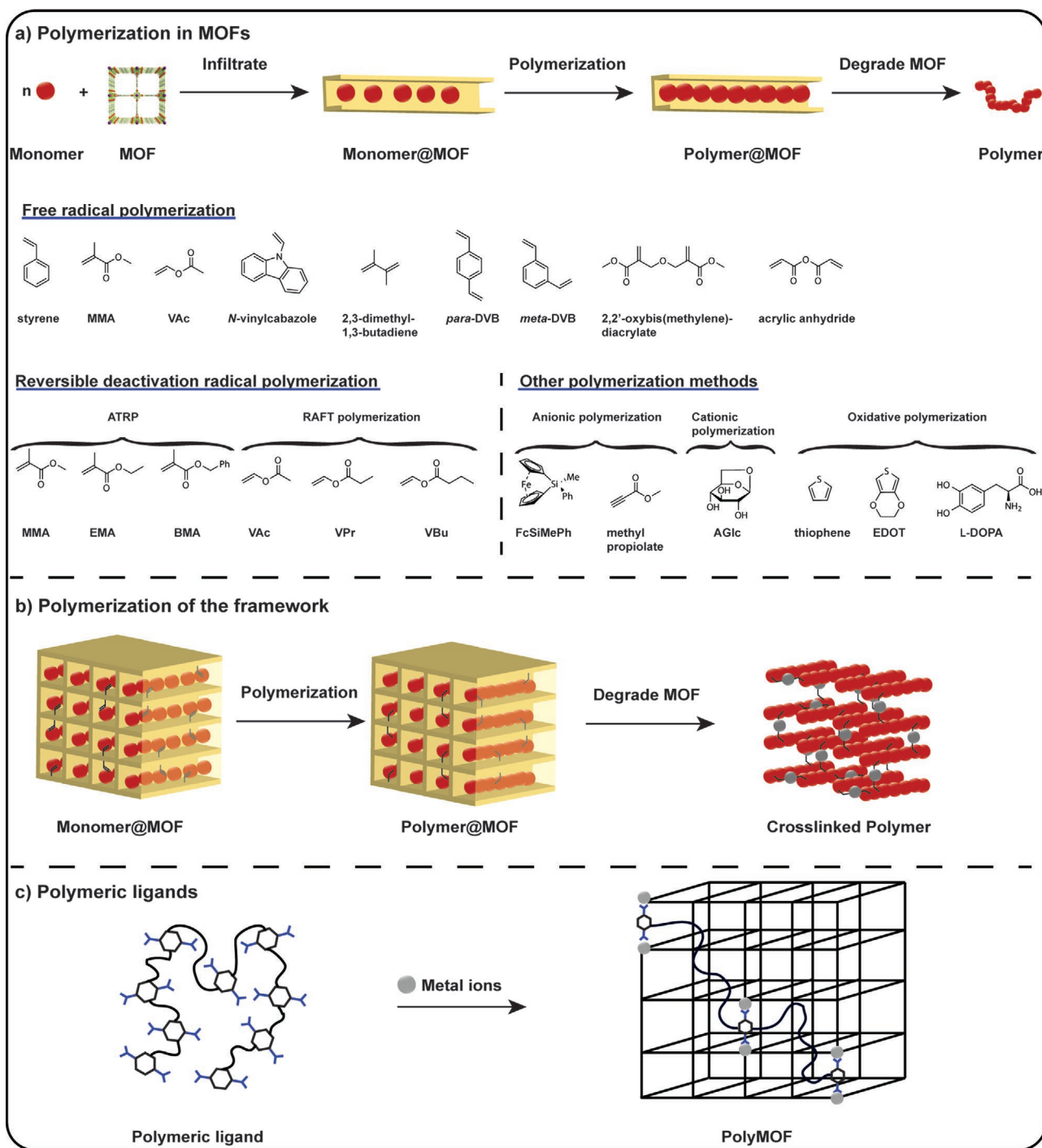


**Figure 3.** Proposed mechanism for the 1,4-*cis*-selective polymerization of 1,3-butadiene with Co(II)-based bis(1H-1,2,3-triazolo[4,5-*b*],[4',5'-*i*])dibenzo[1,4]dioxin-based MOFs. Reproduced with permission.<sup>[61]</sup> Copyright 2017, American Chemical Society.

the channels is an intriguing option to control chain growth processes (Scheme 3), especially regarding stereochemistry. Accordingly, the control over stereochemistry in polymerization reactions inside of MOFs is a topic of significant interest, which mainly addresses control over tacticity. In recent decades, tacticity control has been in the focus of research in polymer chemistry both from a fundamental and an application point of view.<sup>[28,29]</sup> In general, polymerization in MOF pores can be utilized for various purposes. The MOF can be used as sacrificial template in order to obtain polymers with specific architecture or microstructure. Nevertheless, the removal of the MOF template is one of the main disadvantages of polymerizations in MOFs so far as it is less economic than catalytic approaches. It also adds another step of purification that might—depending on the reagents used—alter the polymer structure, for example, the endgroup fidelity. A further approach to complex polymer materials is the polymerization of ligands in the MOF, for example, to form well-defined porous polymers or enhance the stability of the framework against external influences. Another option is the preservation of the MOF for the final application and to form composite materials, which will be covered in Section 4.



**Scheme 3.** Overview of MOFs as polymerization environment: a) Polymerization in MOFs highlighting different polymerization methods, b) polymerization of the framework, and c) polymeric ligands for polyMOF formation. (AGlc, 1,6-anhydro- $\beta$ -D-glucose; BMA, benzyl methacrylate; L-DOPA, L-3,4-dihydroxy-L-phenylalanine; DVB, divinylbenzene; EDOT, 3,4-ethylenedioxythiophene; EMA, ethyl methacrylate; FcSiMePh, methyl phenyl sila[1]ferrocenophane; MMA, methyl methacrylate; VAc, vinyl acetate; VBu, vinyl butyrate; VPr, vinyl propionate).

### 3.1. Radical Polymerization

Certainly, the first option is the investigation of free radical polymerization. As such, Kitagawa and Uemura reported the first example of a polymerization inside of an MOF in 2006, that

is, styrene was polymerized via free radical polymerization.<sup>[69]</sup> Interestingly, rather low  $\bar{D}$  was obtained, which was attributed to less likely bimolecular chain termination events due to the restricted mobility of polymeric radicals in the pores. A further study was conducted by the same team utilizing ligands with



different steric demands to tailor pore geometry in the MOFs and to study the effects of confinement on tacticity.<sup>[70]</sup> Therefore, styrene, MMA, or vinyl acetate (VAc) were introduced in the MOF channels together with AIBN to perform free radical polymerization. Again, rather low  $\bar{D}$  was obtained compared to polymerization in the bulk. More importantly, a relationship between ligand size and tacticity was found for MMA and VAc as increased amounts of *m* diads were detected for more bulky ligands. Notably, no polymerization was observed for very bulky ligands that hindered monomer inclusion. Later on, the free radical polymerization of MMA in MOFs was studied in more detail.<sup>[71]</sup> Accordingly, *bdc*-based MOF ligands were modified in the 2 and/or 3 position and the polymerization analyzed statistically, which revealed occurrence of the penultimate effect in the polymerization inside of MOF channels. In the coming years, the area expanded, for example, styrene sulfonate or *N*-vinylcarbazole were polymerized in MOFs.<sup>[72,73]</sup> Notably, 2,3-dimethyl-1,3-butadiene was polymerized in an MOF as well, which is a monomer that does not lead to high molar mass polymers via classical free radical polymerization due to unfavorable side reactions.<sup>[74]</sup> In the MOF-governed approach polymers with a molar mass around 17–29 kg mol<sup>-1</sup> were obtained. Moreover, the utilization of MOFs with different pore sizes allowed to form polymer with preferred microstructure (1,2 addition, *cis* or *trans*). An avenue to polymer blends was proposed by Uemura. Two consecutive polymerizations of different monomers were performed in an MOF, which had significant impact on the polymer mixing properties. For example, PS was formed in an MOF, the second monomer MMA infiltrated and polymerized again to form an MOF that was filled with two different polymer types (Figure 4).<sup>[75]</sup> Finally, the MOF was removed to reveal a PS/PMMA blend. Usually, polymers of dif-

ferent types tend to demix in the blend forming two distinct polymer phases. In the case of the aforementioned preparation process no demixing was observed and a homogeneous single polymer phase in a kinetically trapped state was indicated that was stable for over 8 months at ambient temperature. Overall, already with the first examples dealing with free radical polymerization only, the polymerization in MOFs showed a remarkable effect on polymer structure and properties.

To improve control over chain end functionality and open up new opportunities via formation of macroinitiators in MOFs, RDRP was attempted by our team. In a first step, ARGET ATRP was performed in a Zn-based MOF. Therefore, methacrylate monomer, initiator, DABCO, and Cu(II) catalyst were infiltrated into Zn<sub>2</sub>bdc<sub>2</sub>DABCO. MMA, ethyl methacrylate (EMA), BMA, and isobornyl methacrylate (IBMA) were utilized as monomers.<sup>[76]</sup> IBMA showed no signs of polymerization in the MOF, which was most likely due to the bulky nature of the monomer that kept the monomer excluded from the MOF pores. The other monomers were converted to polymers featuring a narrow molar mass distribution. In a next step, the MOF was functionalized with initiator to improve control over the polymerization. Thus, polymerizations were conducted in the same way as before but without initiator addition. Polymers with narrow molar mass distribution ( $\bar{D} = 1.1–1.4$ ) and high molar masses up to 392 kg mol<sup>-1</sup> were obtained, which is a remarkable achievement given the usual challenge to yield high molar masses in ATRP. Most likely, the improved control and high molar mass of the obtained polymers can be explained with the MOF environment that hinders termination reactions. Finally, the tacticity of the obtained polymers was investigated via <sup>13</sup>C NMR showing improved tacticity compared to the bulk polymerizations, that is, 10% of *mm* of triads compared to 1% *mm*

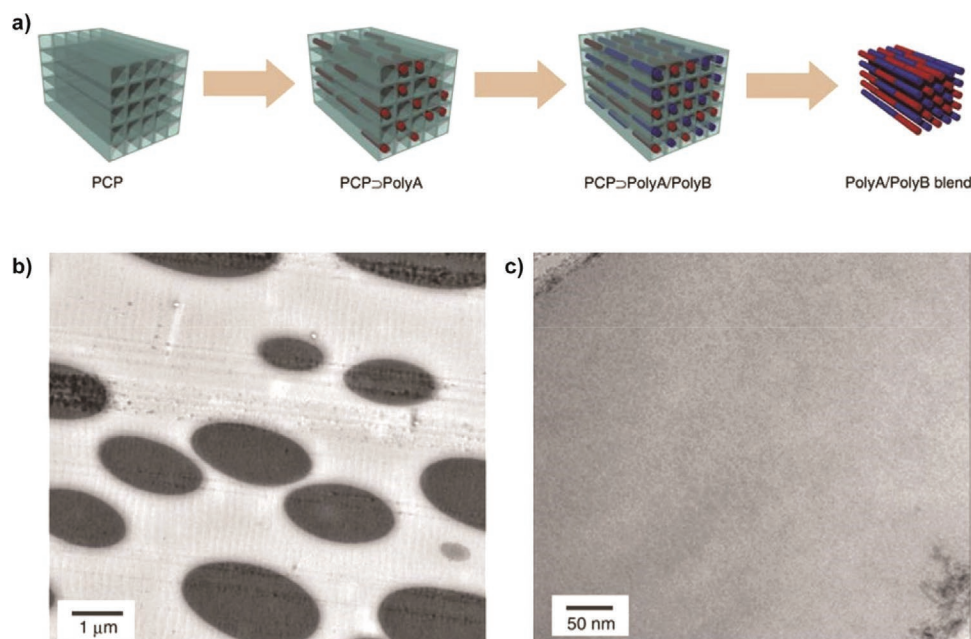


**Figure 4.** Formation of polymer blends in MOFs. a) Schematic overview depicting the formation of polymer A, followed by polymer B and dissolution of the MOF to reveal the polymer blend mixed on a molecular level. TEM image of phase-separated PS/PMMA blend obtained by b) casting from CHCl<sub>3</sub> solution and c) the well-mixed blend isolated from the MOF. Reproduced with permission under the terms of the CC-BY license.<sup>[75]</sup> Copyright 2015, The Authors.



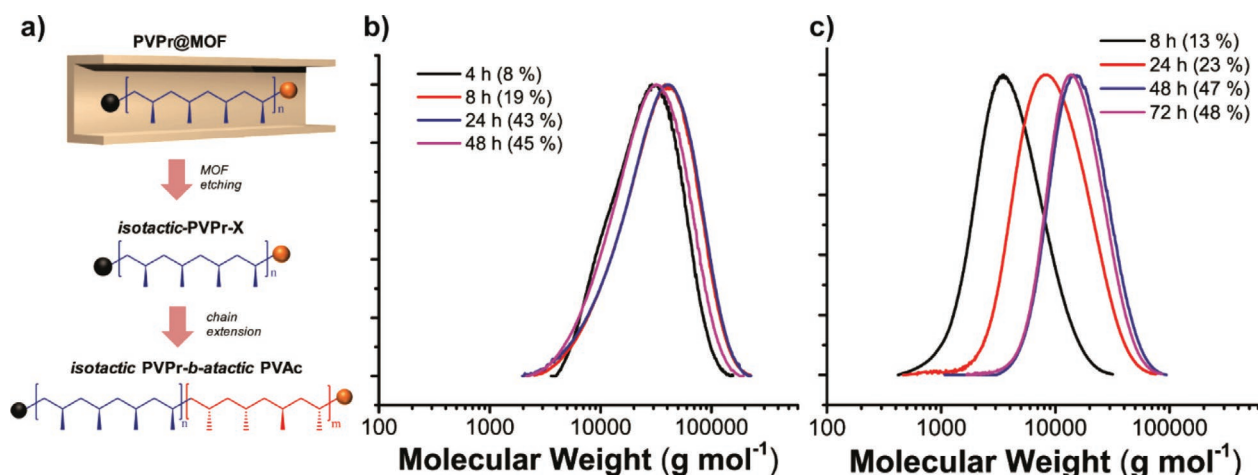


**Figure 5.** a) Schematic overview of the polymer in the MOF pores, release of the polymer, and formation of block copolymers. b) Molar mass distributions of PVPr prepared by free radical polymerization in the MOF, and c) PVPr prepared by RAFT polymerization in the MOF after various reaction times (conversions). Adapted under the terms of the CC-BY license.<sup>[77]</sup> Copyright 2017, The Authors.

triads for the bulk in the case of EMA. Overall, the best tacticity values were obtained for EMA. Most likely, the increased tacticity in EMA is due to a compromise between monomer mobility and steric restriction in the MOF.

Similarly, the RAFT polymerization of vinyl ester monomers in MOF environment has been studied (Figure 5).<sup>[77]</sup> Therefore, Zn<sub>2</sub>bdc<sub>2</sub>DABCO was utilized as environment together with AIBN as initiator and (*S*)-2-(ethyl propionate)-(*O*-ethyl xanthate) as chain transfer agent as well as a free radical polymerization for reference. Polymerization kinetics were investigated to obtain an insight regarding the polymerization mechanism. In the case of free radical polymerization, molar masses were rather constant regardless of monomer conversion. Contrarily, the molar mass increased with raising conversion in the case of RAFT polymerization, which is an indication that a RDRP process took place inside the MOF and block copolymers were synthesized in a second step. Furthermore, tacticity of the formed vinyl ester polymers was investigated after hydrolysis to the corresponding poly(vinyl alcohol) (PVA). In order to obtain information on the effect of steric requirements of the monomer on tacticity, polymerizations of VAc, vinyl propionate (VPr), and vinyl butyrate (VBu) were investigated. Interestingly, an optimum of the *mr* triad content was found for PVA derived from VPr, which is the monomer with intermediate size. This finding is analogous to the case for ATRP and supports the assumption that a compromise between steric restriction and monomer mobility is needed to improve polymer tacticity via polymerization in porous environment. Finally, the combination of MOF-derived polymer with a second block from the bulk polymerization leads to a block copolymer with blocks of different tacticities.

As shown by the polymerization reactions in MOFs, improved control over tacticity or polymer architecture was enabled either via monomer size or pore sizes. Nevertheless, the obtained stereoregularity is far from perfect. Apparently, intermediate monomer sizes lead to enhanced tacticity control, which might be due to the interplay between steric demand of the monomer and mobility in the nanochannel. In principle, a perfect tacticity could be achieved if the monomers align perfectly inside of the

channel and keep in place for the course of the polymerization. To keep the monomers in place the molecule should be bulky enough to fit perfectly into the channel. In reality, some space is needed to align the monomers and as such a perfect alignment is hard to achieve. In the case of free radical polymerization decent control over the molar mass distribution was obtained, that is, a limited occurrence of termination reactions due to the decreased probability of end chain radicals to meet. The question arises how the RDRP polymerizations in MOF works from a mechanistic point of view. Usually the common RDRP mechanisms involve reactions at the chain end of the polymers. Therefore, a polymerization according to the traditionally proposed RDRP mechanisms can be doubted at least as these mechanisms need additional molecules to be present to reversibly activate the chain ends. Such reversible ongoing reactions at the chain end seem unlikely as the approach of reactants is sterically hindered inside of the pore. It seems to be more probable that an active chain polymerizes for a long time before it is deactivated. At this point it meets the starting point of another chain and the respective molecule/atom to deactivate the radical. Nevertheless, at the current point in time no specific evidence for the actual mechanism of RDRP in MOFs has been figured out.

The confinement effect was also utilized to control the polymer architectures of multifunctional monomers, for example, *para*- or *meta*-divinylbenzene (DVB).<sup>[78]</sup> In the bulk or in solution, a crosslinked network is obtained, while in MOFs with pore sizes around 0.8 nm linear polymers can be obtained. In this case, the framework flexibility also plays a significant role. For example, *meta*-DVB could be polymerized in a rigid framework and *para*-DVB did not polymerize. In the case of a flexible framework, *para*-DVB could be polymerized as the environment could adopt to the geometry of the monomer and allow propagation. Notably, the architecture could be tailored with pore size, that is, branched structures of *para*-DVB were obtained for pore sizes around 1.1 nm. A similar effect was observed for 1,6-diene monomers, namely dimethyl 2,2'-[oxybis(methylene)]diacrylate and acrylic anhydride.<sup>[79]</sup> Hence, branched structures were formed in solution but linear

cyclopolymerization products were formed in the MOF. As such not only the polymer architecture but also the polymerization product formation was controlled, that is, selective formation of cyclopolymerization product.

In addition to the pore size, MOF chemistry can be altered as well, for example, by Uemura and coworkers to alter the polymerization of MMA. Therefore, Al(III), Eu(III), Nd(III), Y(III), La(III), or Tb(III) 1,3,5-benzenetriscarboxylate MOFs were utilized that contain coordinatively unsaturated metal sites.<sup>[80]</sup> Interestingly, significant influences from the unsaturated sites on the polymerization product were found, that is, polymer yield, tacticity, and molar mass. For example, the isotactic and heterotactic triads increased in comparison to the bulk and a conventional MOF. Moreover, the control over tacticity could be correlated with the Lewis acidity of the unsaturated metal sites leading to a stronger change in tacticity with higher Lewis acidity and the best results for Tb(III). Later on, copolymerization of styrene and MMA was studied.<sup>[81]</sup> In comparison to the case of bulk copolymerization of MMA and styrene, copolymers with increased MMA fraction could be obtained in the MOF. The effect was attributed to the varied monomer reactivity due to coordination of MMA and unsaturated metal sites. Interestingly, the effect was not observed at elevated temperatures, probably due to weakened interactions of MMA and the MOF ligands.

### 3.2. Other Polymerization Methods

In addition to radical polymerization, other polymerization methods were utilized as well in order to obtain polymers in MOF channels. While radical polymerization in MOFs constitutes the most significant part of the literature, probably due to the convenient reaction conditions, other polymerization mechanisms obtained increasing attention recently. The utilization of other polymerization methods is mainly driven by two factors.

First of all, polymers/polymer structures can be generated that are not accessible otherwise. Secondly, structured materials for specific applications can be fabricated, for example, for organic electronics. For example, a silicon-bridged [1]ferrocenophane, that is, methyl phenyl sila[1]ferrocenophane (FcSiMePh), was polymerized in MOFs as shown by Manners and Uemura.<sup>[82]</sup> Thermal ROP of FcSiMePh led to polymers with increased isotactic content and no cyclic impurities that showed slightly changed redox coupling properties compared to bulk-derived material. Another example is the formation of poly(acetylenes) in MOFs. Therefore, C–H acidic methyl propiolate was introduced into an MOF with basic oxygen atoms and acetylene coordination sites.<sup>[83]</sup> The polymerization was initiated via the deprotonation of the acidic acetylene and propagation led to stereoregular polymers, that is, selective *trans*-product formation due to the narrow channel size was observed. An example of particular interest is the formation of poly(glucose) via cationic ring-opening polymerization of 1,6-anhydro- $\beta$ -D-glucose (AGlc) (Figure 6).<sup>[84]</sup> Due to the confined polymerization environment a soluble linear polymer is obtained, while in solution branched and insoluble structures are generated. As such a linear poly(saccharide) was formed via a chain growth mechanism leading to a polymer structure that is impossible to synthesize otherwise without protection group chemistry.

Oxidative polymerization has been performed in MOFs as well. The synthesis of conducting polymers inside of MOF pores leads to isolated molecular wires, which is of significant interest in basic organic electronics research as shown by Uemura and coworkers.<sup>[85]</sup> Due to the polymerization in the MOF, well-aligned poly(thiophene) (PT) was synthesized that showed a remarkable conductivity of three orders of magnitude higher than solution-derived PT after removal of the MOF template. A combination of PT and fullerenes was described as well.<sup>[86]</sup> Therefore, C<sub>60</sub> was introduced in a MOF followed by terthiophene that was polymerized subsequently in an oxidative polymerization. As such a donor acceptor interface was

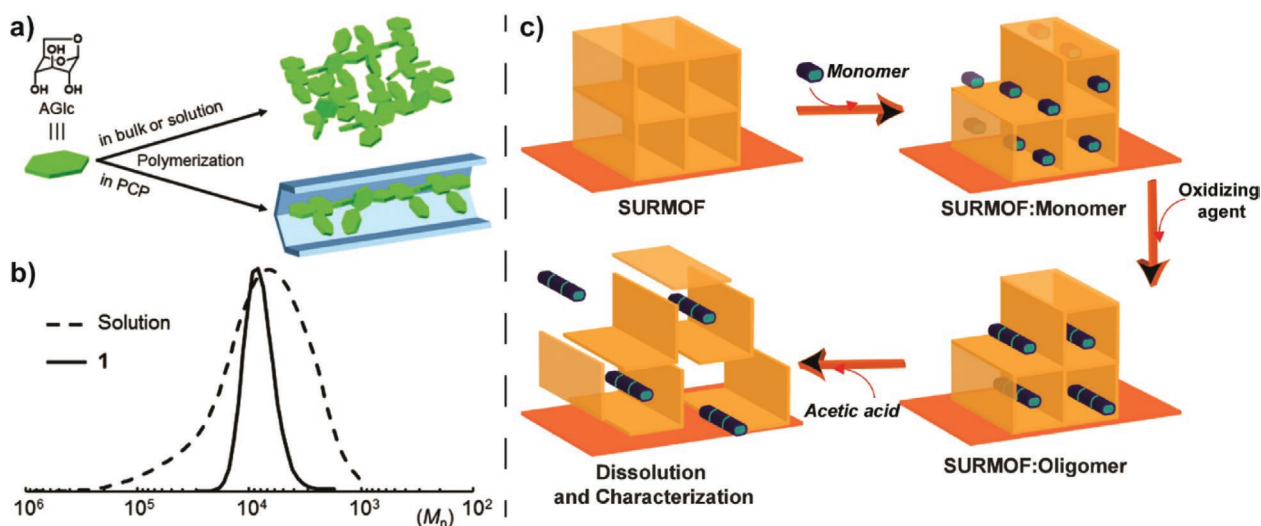


**Figure 6.** a) Polymerization of 1,6-anhydro- $\beta$ -D-glucose (AGlc) in bulk, solution, or in La(1,3,5-benzenetriscarboxylate)(H<sub>2</sub>O) MOFs. b) SEC profiles of PAGlc synthesized inside of a MOF (solid line) or in DMF solution. Reproduced with permission.<sup>[84]</sup> Copyright 2016, Royal Society of Chemistry. c) Schematic overview of the encapsulation of terthiophene monomers and the oligomer formation inside the nanopores of SURMOF-2 via oxidative polymerization. Reproduced with permission.<sup>[87]</sup> Copyright 2018, Elsevier.

generated directly in the MOF channel featuring an end-on contact of PT and  $C_{60}$ . Wöll and coworkers synthesized PT as well, albeit surface anchored MOF films were utilized, namely SURMOF-2 (Figure 6).<sup>[87]</sup> The authors synthesized poly(3,4-ethylenedioxythiophene) (PEDOT) inside of surface anchored MOFs as well. In a similar way, Smoukov and coworkers synthesized PEDOT inside of an MOF mounted on a poly(pyrrole) (PPy) surface.<sup>[88]</sup> After removal of the framework, PEDOT nanostructures were obtained with conductivity similar to bulk PEDOT. Moreover, flexible films were fabricated that are of interest for future applications in portable electronics.

The formation of nanostructured poly(aniline) (PANI) via MOF templates was investigated by Qiu and coworkers.<sup>[89]</sup> In order to do so, a MOF layer, for example,  $Zn_2(bdc)_2$ DABCO, MIL-68, or HKUST-1, was prepared on a layer of PANI. The primary PANI layer was needed to improve conductivity for the subsequent electropolymerization of aniline inside of the MOF pores and to introduce a tight binding between MOF and electrode via hydrogen bonding. In the next step aniline was infiltrated into the MOF pores and electropolymerized to mimic the porous MOF structure. Finally, the MOF scaffold was removed to reveal nanoporous PANI with well-defined pore structures and improved surface area. In a similar way, Zhang and coworkers utilized HKUST-1 mounted on a surface as template for the oxidative polymerization of L-3,4-dihydroxy-L-phenylalanine (L-DOPA).<sup>[90]</sup> After etching, a porous homochiral poly(L-DOPA) film was obtained that could be utilized to separate *R/S* naxroxen with an enantioselectivity of 32%.

### 3.3. Polymerization of Framework Ligands and Utilization of Polymeric Ligands

The polymerization of monomers inside of MOF structures can be extended to the ligands, that is, the polymerization of the ligands in the pore walls. As such, the MOF can be used as a template to place monomer units specifically in space and thus control the polymerization in a spatial way. Recently, Uemura and coworkers achieved the first example of sequence controlled polymerization inside an MOF.<sup>[91]</sup> Therefore, a strategy combining polymerization in MOF pores and polymerization of MOF ligands was employed. At first an MOF was formed with mono vinyl functionalized ligands. After infiltration of additional free monomer in the pores, a polymer could be generated via free radical polymerization. Due to the placement of a monomer in the framework and monomer in the channel an alternating sequence of ligand-derived monomer and infiltrated monomer was obtained. As such, the structural control in the MOF via ligand placement in the crystal lattice was translated into a sequence specific polymer. In a similar way, Sada and coworkers performed an A–A/B–B step growth polymerization between MOF ligands and incorporated monomers (Figure 7).<sup>[92]</sup> Therefore, an MOF was fabricated from  $Zn^{2+}$  and a ligand that contains two azide functions (Aztptdc). In the next step, a double alkyne functional monomer (CL2) was introduced together with Cu(I) catalyst to perform CuAAC. In contrast to conventional step growth polymerization, the polymerization was rather insensitive to the stoichiometry, which can be explained with the spatial controlled placement

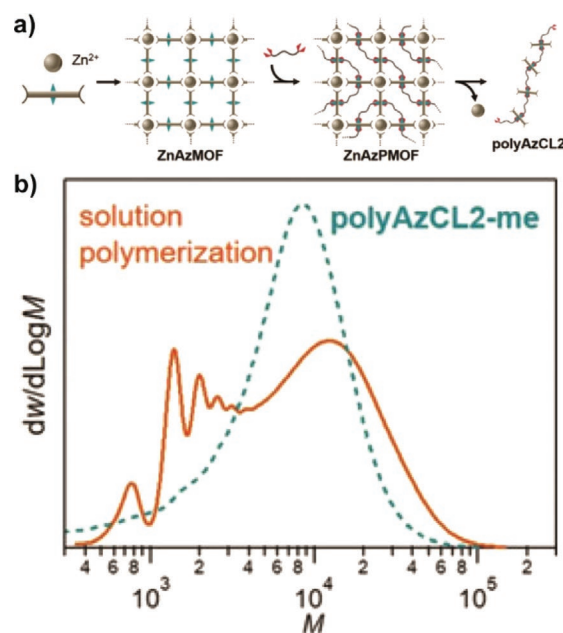


**Figure 7.** a) Scheme of the polymerization of Aztptdc and CL2 in ZnAztptdc MOF and subsequent decomposition of ZnAzP MOF to obtain linear polymer. b) SEC evaluation of the product from solution polymerization (orange line) and from the MOF (green line). Reproduced with permission.<sup>[92]</sup> Copyright 2019, Wiley-VCH.

of one of the monomers in the MOF and the non-equilibrium situation inside of the pore channels. The degree of polymerization (DP) was depending more significantly on the monomer arrangement, that is, the crystal structure, then on stoichiometry. As such, the result is quite remarkable as it contradicts the traditional rules of step growth polymerization and shows the power of confined space in polymerization processes. Vittal and coworkers reported the formation of syndiotactic polymers via polymerization of MOF ligands via photochemical [2 + 2] cycloadditions.<sup>[93,94]</sup> Accordingly, a Zn(II)-based MOF was synthesized via the ligands 4,4'-oxybis(benzoic acid)—forming a plane—and 1,4-bis[2-(4'-pyridyl)ethenyl]benzene (bpeb)—forming pillars. The pillar ligands were designed to contain two double bonds for photopolymerization. Due to the steric requirements of the MOF and the stereochemistry of the cycloaddition, syndiotactic polymers were obtained.

Another option is the utilization of ligands with multiple polymerization sites to obtain crosslinked materials. As such, various stable polymer structures can be formed via MOF templating to translate the well-defined specific pore structure of the MOF into a polymer material. For example, Vittal and coworkers crosslinked an MOF with the aforementioned bpeb ligands in a tetrahedrally coordinated Zn(II) MOF.<sup>[95]</sup> To that end, a slight change in the ligand composition allowed to change the obtained material completely, that is, terephthalic acid was utilized instead of the bent 4,4'-oxybis(benzoic acid). Thus, a diamondoid MOF network was obtained that could be crosslinked completely with UV light to obtain a stable polymer material retaining the microporosity of the parent precursor. Another variation was observed in the case of formic acid introduction.<sup>[96]</sup> A MOF with twofold interpenetrated network CdS



topology was obtained that underwent a single-crystal to single-crystal transformation after UV light irradiation.

Yang and coworkers utilized a photochemical [2 + 2] cycloaddition of ligands and guests in the MOF to form a crosslinked network.<sup>[97]</sup> Therefore, a Mn(II) MOF formed via the 1,3-phenylenediacrylic acid ligand was infiltrated with bpeb and irradiated with UV light. To understand the photopolymerization process the solid material was studied in situ with X-ray crystallography. Three processes were observed, that is, polymerization, dimerization, and pedal-like isomerization. Finally, a distorted but intact crosslinked MOF was obtained. A box-like structure was described by Sada and coworkers, who formed an unfunctionalized cubic MOF and covered it with another layer of MOF including reactive azide functional ligands.<sup>[98]</sup> After infiltration of a tetra alkyne compound, CuAAC was performed to obtain cubic structures with MOF core and crosslinked MOF outer layer. Finally, the MOF core was removed to reveal a box-like cubic polymer structure. In a similar way, the same team fabricated well-defined polyelectrolyte gel architectures via CuAAC-mediated crosslinking of MOF precursors.<sup>[99]</sup> For example, shapes like cubes or octahedra could be generated with that strategy.

Recently, the concept was extended toward modular programming of MOFs by Zhou and coworkers (Figure 8).<sup>[100]</sup> Therefore, an MOF system was designed that contained independent modules. As such, each module could be modified without affecting the other modules. Sequential click reactions and acid treatment were utilized to modify an MOF into a polymer, while keeping another MOF in the multivariate system untouched. At first a simple module was designed employing a Zr-based MOF (PCN-222) and Zn-based Aztpc MOF that could be crosslinked via CuAAC. The Zr-MOF is rather stable in acidic conditions, while the Zn-MOF readily hydrolyzes. As such, the individual parts responded selectively on external chemical pH stimulus. Crosslinking of the weak Zn-framework and pH treatment allowed the preservation of the overall structure. Moreover, the amount of the individual modules in the composite could be tailored as well as placed in a spatially controlled way. Finally, a third module was added, that is, HKUST-1, that again shows a different stability. After crosslinking, HKUST-1 could be selectively removed via acid treatment to leave a hollow space. Overall, the system reacted to external stimuli and the structure of the MOF hybrid could be switched in a modular way. Thus, the obtained MOF featured a way to imprint its chemical history into the system.

Tsotsalas and coworkers utilized thiol-ene photopolymerization to crosslink a SURMOF formed from ligands with allyl functionalization.<sup>[101]</sup> Due to the photopolymerization approach after introduction of trithio molecules, the MOF structures could be crosslinked in a spatial way. After removal of the MOF template, defined porous polymer structures were obtained on the surface. In another study, the utilization of polymerizable ligands was employed by Uemura and coworkers to form crosslinked polymer materials with unique shapes.<sup>[30]</sup> MOFs were synthesized that contained a significant amount of 2,5-divinyl-terephthalic acid instead of terephthalic acid. After infiltration of free monomer and radical polymerization, a crosslinked material was obtained that was stable after the

removal of metal ions and remaining ligands. Moreover, the crosslinked pure polymer material featured the shape and pore structure of the MOF template with improved thermal and mechanical properties compared to the bulk-derived polymer. Song and coworkers utilized a Cu(II)-*para*-phenylenediamine MOF as template to form spherical poly(*para*-phenylenediamine) particles.<sup>[102]</sup> Cu(II) acted not only as structure directing agent but also as polymerization reagent at the same time to induce the oxidative polymerization of *para*-phenylenediamine. At first, cube-like crystallites were formed that assembled to hollow spherical particles over time. During the preparation, the formed MOF superstructure particles converted into polymers and at the same time Cu(II) was reduced to Cu<sub>2</sub>O and finally Cu under solvothermal conditions. In such a way, structures of polymer materials with unprecedented shapes were generated.

Furthermore, there is the option of the utilization of polymers as ligands to start from, which leads to so-called poly-MOFs. As such, rather flexible polymers are utilized, for example, containing 5–8 carbon alkyl spacers in the backbone, to accommodate crystal formation, which was pioneered by Cohen and coworkers.<sup>[103]</sup> For example, Zn(II) was combined with a polyether containing a benzene dicarboxylic acid as free acid in the backbone. The acid functions acted as ligand toward Zn(II). Interestingly, although an amorphous polymer was utilized, crystalline and porous MOFs were obtained. Nevertheless, the obtained crystals were polycrystalline, which was probably due to intergrowth of various crystallites via sharing of polymers between individual crystallites. Moreover, the materials comprised increased hydrophobicity depending on alkyl chain length. Therefore, increased stability against moisture compared to reference MOF-5 was obtained. Altogether the properties of the MOF and polymers could be nicely combined in that way making them more durable for future applications. Later on, the concept was extended toward more complex structures, for example, via combination with small molecule ligands and other metal ions.<sup>[104]</sup> The incorporation of different ligands facilitated the formation of plate-like particles or hexagons in contrast to previously obtained cubic morphologies. PolyMOFs were also formed based on the common Universitet i Oslo-66 (UiO-66) MOF via utilization of Zr(IV), which enabled the formation of remarkable crystal morphologies with hierarchical porosity.<sup>[105]</sup> More importantly, the morphology could be controlled via the spacer length in the polymer. In a subsequent study, the ligands in the polymer backbone were modified for isorecticular expansion.<sup>[106]</sup> Polymer precursors obtained from acyclic diene metathesis (ADMET) polymerization were utilized. The porosity could be controlled via the incorporation of different dicarboxylic acids, namely based on benzene, biphenyl, and terphenyl, which allowed isorecticular expansion of the polyMOFs and addresses a common feature of classical MOF materials.

Recently, Cohen and coworkers studied the effect of block copolymers on crystal morphology for MOF-5 and UiO-66 (Figure 9).<sup>[107]</sup> Hence, the crystal size could be controlled via the length of the non-coordinating block due to hindered aggregation of crystallites in the case of longer non-interacting blocks. MacLeod and Johnson studied the formation of polyMOFs from block copolymers as well.<sup>[108]</sup> Therefore, a well-defined



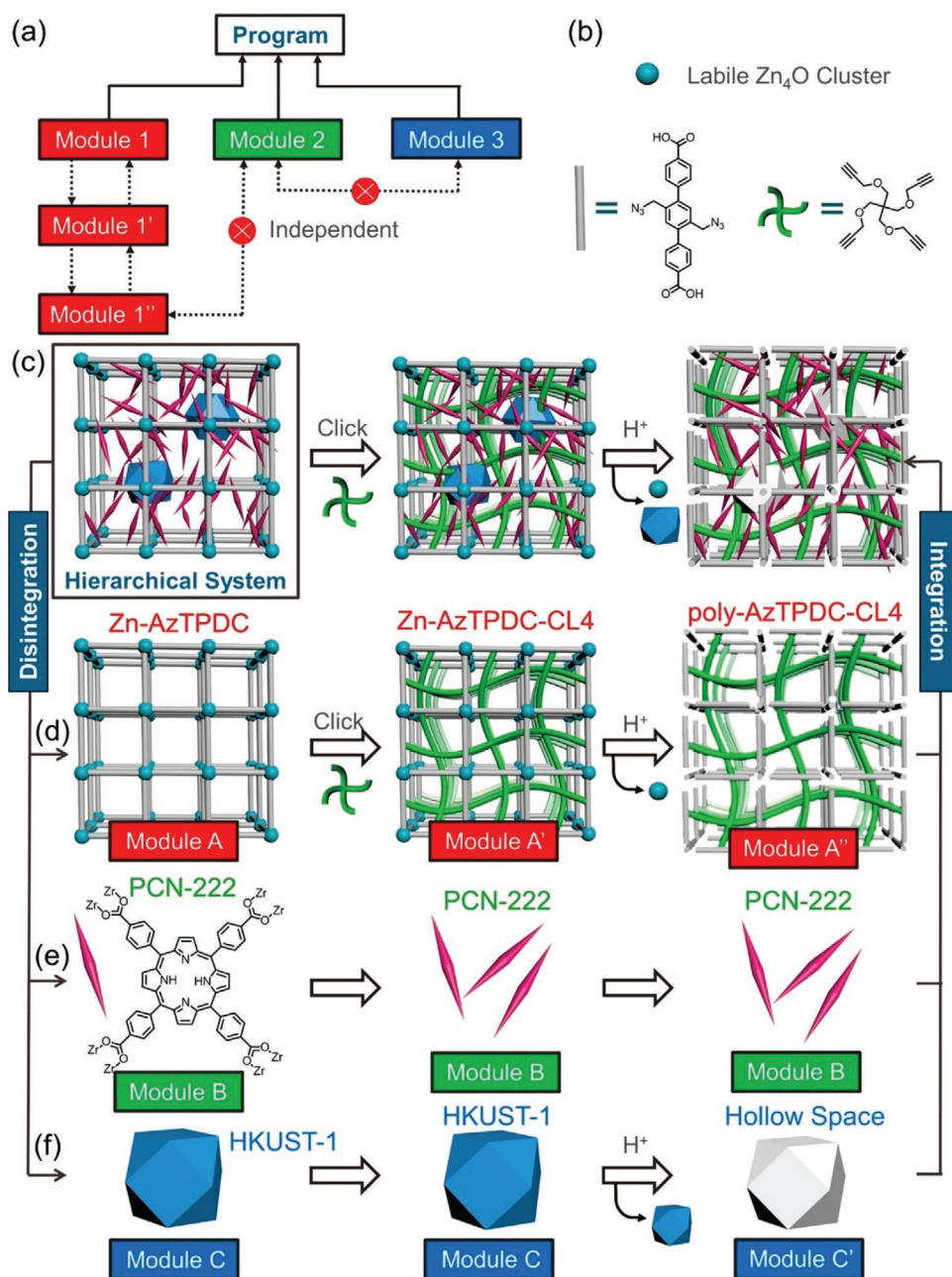


**Figure 8.** Schematic overview of modular multivariate MOF structures. a) The concept of modular programming; b) building blocks for the construction of Zn-Aztpdc MOF; c) synthesis of the modular composite containing modules A, B, and C; d) synthetic pathways and transformation with the Zn-Aztpdc (A) module (A to A' via CuAAC; A' to A'' via acid treatment and metal ion removal); e) the PCN-222 module (B); the HKUST-1 module (C), and transformation chemistry (C to C' via acid-mediated removal). Reproduced with permission.<sup>[100]</sup> Copyright 2019, American Chemical Society.

interacting block based on benzene dicarboxylic acid was utilized that was connected to PS via CuAAC. A combination with Zn(II) ions led to the formation of polycrystalline MOF particles with dimensions in the nanometer range in a PS matrix. This example points toward significant development options for MOF/polymer combinations with respect to complex material architectures. Overall, the utilization of polymeric ligands opens up new opportunities for complex MOF architectures as well as improves the properties and introduction of adjustability.

#### 4. MOF-Polymer Hybrid and Composite Materials

The process of polymerization in MOFs is not only useful for the preparation of polymers with unprecedented architectures, tacticity, or control over properties but also for the preparation of hybrid and composite materials.<sup>[109–111]</sup> In such a way, the properties of MOFs and polymers can be combined or even extended, as already mentioned regarding the class of poly-MOFs. In general, the strategy of composite formation is utilized to fabricate materials that combine the properties of both

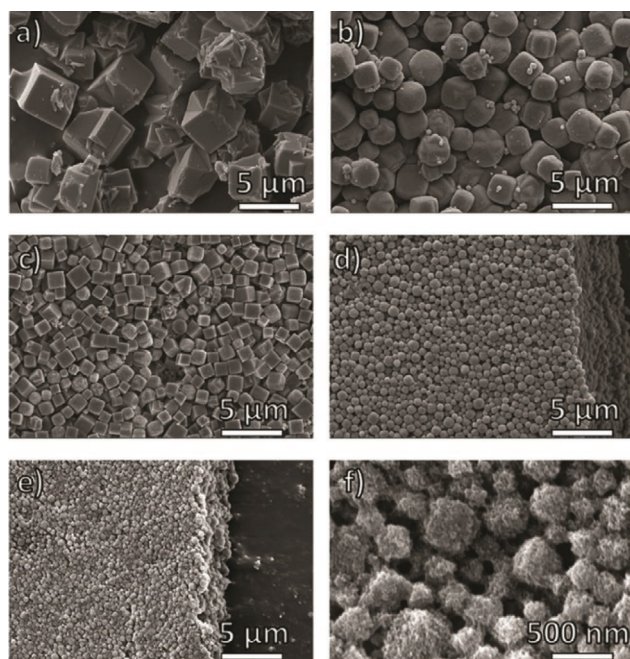
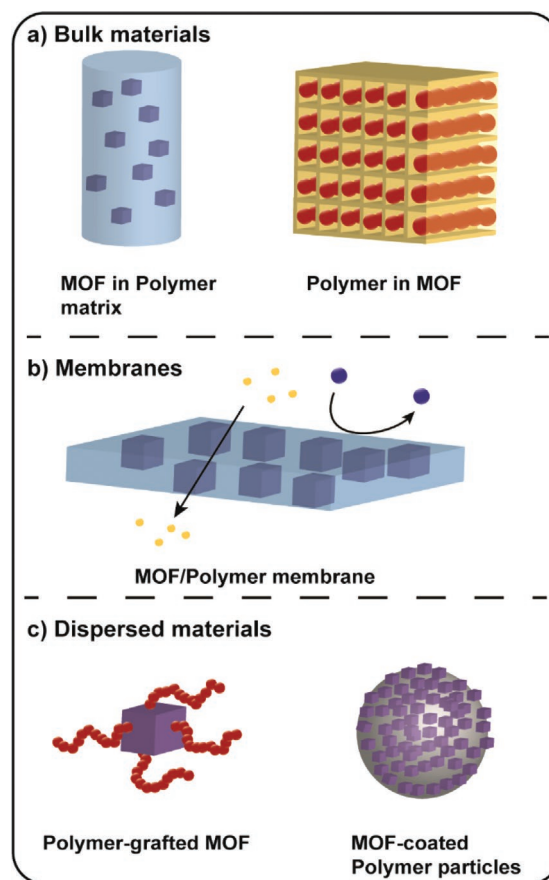


**Figure 9.** SEM images of polyMOF-5 prepared from bdc-based polymer ligands (Pbdc). a) Pbdc; b) Pbdc-*b*-PEG<sub>2k</sub> (2%); c) Pbdc-*b*-PEG<sub>4k</sub> (1%); d) Pbdc-*b*-PEG<sub>2k</sub> (20%); e,f) Pbdc-*b*-PEG<sub>4k</sub> (10%). Reproduced under the terms of the CC-BY license.<sup>[107]</sup> Copyright 2019, The Authors.

constituents. In a lot of cases, hybrid formation is achieved, where the obtained material features new properties that exceed the sum of the individual components. In the realm of MOF research, properties like catalytic activity or porosity from MOFs can be combined with processability, solubility, or stimuli response from polymers. Although MOF/polymer hybrids and composites introduce a plethora of opportunities for the fabrication of complex materials with tailored properties, one has to consider the disadvantages as well. For example, metal ions are introduced into the material, which might have negative impact on some biomedical applications. Moreover, the improved complexity is accompanied by more complicated or multistep fabrication procedures.

In order to obtain decent hybrid and composite materials, the compatibility of MOF and polymer is of utmost importance. As studied theoretically by Maurin via force field and quantum chemical computations the compatibility of MOF and polymer strongly depends on polymer rigidity.<sup>[112]</sup> Less stiff polymers—with Young's modulus less than 1 GPa—can interact with the MOF surface more thoroughly, that is, cling to the rough surface and even penetrate the pores partially. On the other hand, stiff polymers have a lower tendency to interact with the MOF surface. With the broad range of MOF/polymer hybrids and composites available, the classification of the materials into useful categories has to be considered. In general, there are several ways to sort MOF hybrid and composite materials. For example, according to the way of combination, for example, infiltration of polymers in MOF pores, grafting of polymers to/from the MOF surface, embedding of MOFs in polymer matrices, or a combination of the approaches. Another option is to classify according to intended application, for example,



**Scheme 4.** Overview of common MOF/polymer hybrid materials. a) Bulk materials, b) MOF/polymer membranes, and c) dispersed materials.

with respect to drug delivery, catalysis, gas adsorption, or conductivity. Certainly, the diversity of the area of MOF-polymer combination is already obvious from these classifications. A straightforward way to categorize MOF-polymer hybrids and composites is according to their physical state, that is, as bulk material or in a particle/dispersed state (Scheme 4). Of course, the physical state is also connected with the intended application. Therefore, in the following section MOF-polymer hybrids will be ordered according to their physical state and further regarding similar applications.

#### 4.1. Bulk Materials

A topic of increasing interest is the combination of MOFs with polymers as hybrid materials in the bulk, for example, for film formation, hierarchical porous materials, or 3D printing. Hence, novel material properties are sought after as well as improvement of existing properties and applications. Overall, a broad variety of polymer/MOF hybrids are described in the literature and various applications are addressed, for example, adsorption, capture, or degradation of various compounds as well as the formation of material with complex 3D shapes. Next to tacticity and polymer architecture, other polymer properties can be addressed via polymerization in MOFs as



well, which is a straightforward way to obtain MOF/polymer hybrids. For example, Kitagawa and Uemura studied the behavior of PS inside of MOF nanochannels and indicated a missing glass transition temperature.<sup>[113]</sup> Moreover, further studies revealed unprecedented behavior of the PS chains showing homogeneous side-chain mobility and relatively low activation energy, which was related to the linear extension of the chains in the pore and the exclusion of chain–chain interactions as they are present in the bulk material. In the case of PEG, also significant effects of the MOF surrounding the thermal transition processes were observed, that is, a reduction of the thermal transition temperature.<sup>[114]</sup> In addition, the observed effect could be tailored via the utilization of different ligands in the MOF structure. The defined pore structure of MOFs can be further utilized to sort polymers with different endgroups. Hence, Uemura and coworkers showed a separation of PEG according to endgroups based on steric hindrance via a rigid MOF structure, that is, trityl and hydroxy endgroups could be separated (**Figure 10**).<sup>[115]</sup> Moreover, the utilization of a flexible MOF allowed for the kinetic separation of  $\alpha$ ,  $\omega$  methoxy, ethoxy, butoxy, and hydroxy endgroups as well as  $\alpha$

hydroxy/ $\omega$  methoxy endgroups due to slight differences in polarity.

On the contrary, polymers can also have an effect on MOF properties. For example, the insertion of polymers is not only useful for separation tasks but also for the mechanical properties of the MOF material. Uemura and coworkers showed significantly enhanced resistance of MOFs against pressure when polymer chains were present in the pores.<sup>[116]</sup> Notably, the enhancement effect showed anisotropic behavior as the polymer chains are aligned in a 1D fashion inside of the pores. In addition to mechanical properties the pore structure can be tailored via polymers as well. Infiltration of monomer and polymerization to a defined conversion can lead to an increase in pore sizes if flexible MOFs are utilized.<sup>[117]</sup> The formation of a polymer chain leads to a deformation of the pore, which is translated through the whole network due to the crystalline nature of MOFs. To prove the applicability of the approach, the respective MOF was utilized for gas adsorption, which was impossible with the precursor MOF. In a similar way, Matzger and coworkers polymerized styrene inside of MOF-5, which increased the CO<sub>2</sub> adsorption capacity due to the distortion of

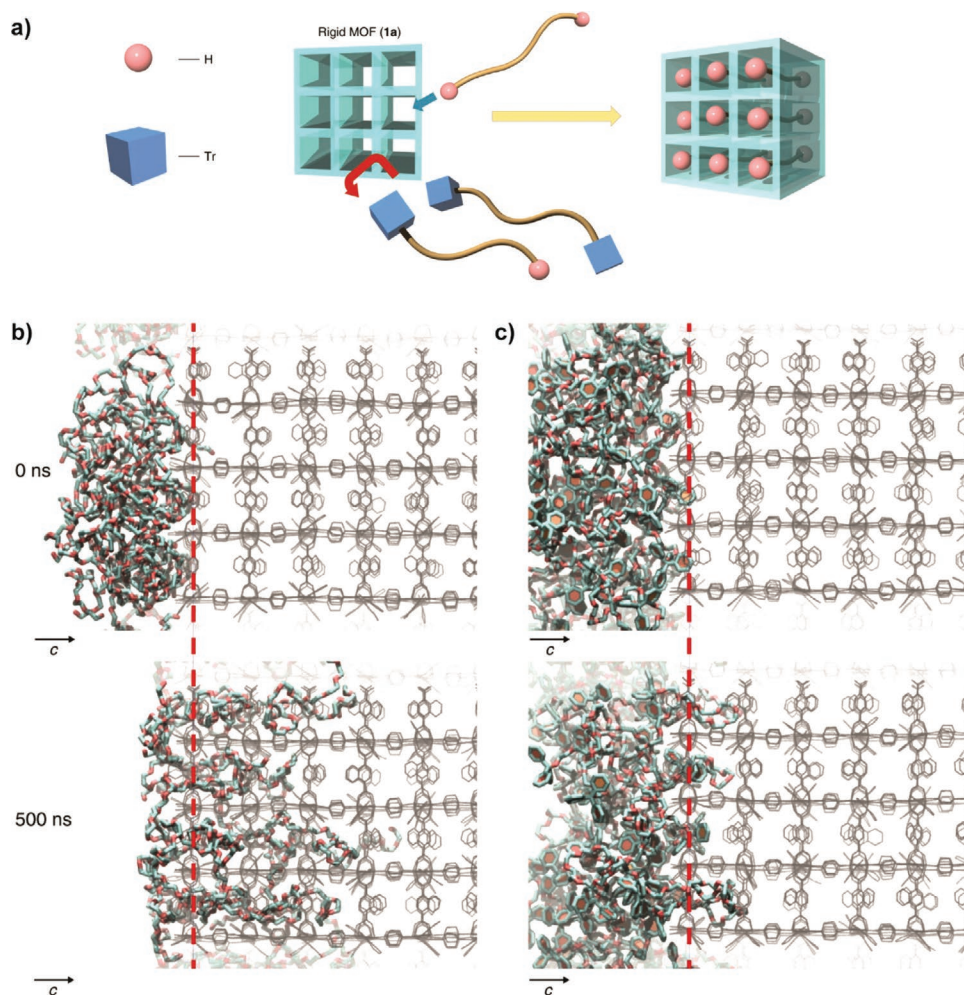


**Figure 10.** a) Use of an MOF for PEG separation. Molecular dynamic simulation snapshots of a MOF with b) H–PEG–H and c) trityl–PEG–trityl at 373 K. Reproduced under the terms of the CC-BY license.<sup>[115]</sup> Copyright 2018, The Authors.

the pore environment.<sup>[118]</sup> Moreover, the stability of the MOF material against hydrolysis was improved.

A way to obtain spatially structured materials is the combination of MOFs and polymers in emulsion templating processes. For example, polymer/MOF composites with macroporous structure can be obtained via the utilization of high internal phase emulsions (HIPEs). As such, monomer and crosslinker are introduced into the continuous phase of a HIPE to obtain a macroporous support material. Bradshaw and coworkers utilized HIPE-based poly(acrylamide) (PAAm) beads as scaffold for the crystallization of MOFs inside of the macropores.<sup>[119]</sup> Similarly, Kovačič and coworkers formed polyHIPE with metal oxide nanoparticles in the walls that acted as metal ion reservoir for MOF growth after addition of ligand.<sup>[120]</sup> Shirshova and coworkers studied the formation of polyHIPE/MOF composites based on MMA and VAc. Polymer and MOF were formed at the same time in one step.<sup>[121]</sup> Later on, Bradshaw and coworkers utilized HIPEs to form macroporous polymer scaffolds as support for various MOFs including catalytically active ones.<sup>[122]</sup> Therefore, a water in styrene/DVB emulsion was prepared featuring MOF particles in the water phase. After polymerization, a microporous material with MOF crystals located at the pore walls was obtained. Moreover, the shape could be tailored via specific molds leading to mechanically durable materials. Finally, the ZIF-1-based material was utilized as catalyst for the Knoevenagel reaction. In a similar way, an MOF/polymer hybrid material featuring magnetic separation was described.<sup>[123]</sup> At first a macroporous PAAm scaffold with Fe<sub>3</sub>O<sub>4</sub> embodiment was synthesized via oil/water emulsion templating. Subsequently, various MOF types were grown in the PAAm scaffold. At last, the HKUST-1 containing macroporous PAAm sample was utilized to study the isomerization of  $\alpha$ -pinene oxide, which showed higher conversion and selectivity compared to bulk HKUST-1. Moreover, the catalyst could be recovered easily via magnetic field.

Queen and coworkers utilized an emulsion method to obtain MOF/polymer composites as well.<sup>[124]</sup> Thus, a Ni-based MOF was dispersed together with dopamine (DA) in the water phase of a hexane/water emulsion and DA polymerized via an oxidation pathway. PDA/MOF composite particles were obtained after solvent removal that showed remarkable CO<sub>2</sub> and water adsorption behavior. Porous MOF/polymer monoliths formed from chitosan and UiO-66 were described by Zhang and coworkers.<sup>[125]</sup> Notably, an ice templating method was utilized to introduce macropores for enhanced mass transport as the monoliths were intended for waste water treatment. Subsequently, methylchlorophenoxypropionic acid—a herbicide with high toxicity—was adsorbed from diluted aqueous solution in the monoliths with significant success. Rzayev and coworkers formed MOF/polymer monoliths via crosslinking of individual MOF crystals with a ligand containing polymer, that is, a polyamide that contains bdc with free carboxylic acid groups in the backbone.<sup>[126]</sup> As such, the bdc units in the backbone could undergo attractive interactions or ligand exchange with the MOFs to form a stable network. As the ligand exchange and attraction was limited to the surface of the MOF crystals, the porous structure of the MOFs was not altered and MOF loadings up to 80% were achieved.

As mentioned before, the synthesis of conjugated polymers inside of MOF pores is a useful way to obtain defined conjugated polymers, for example, in the case of PT.<sup>[85]</sup> While the removal of the MOF template leads to defined conjugated polymers or nanoarchitectures, the combination of conjugated polymers and MOFs can be exploited in a material directly without removal of the MOF confinement as well. In such a way, molecular wires can be obtained as the MOF scaffold hinders interaction of the individual conjugated polymer strands, which might lead to promising electrical properties. Kitagawa reported an avenue to form PT inside La(1,3,5-benzenetrisbenzoate) MOFs.<sup>[127]</sup> Usually, PT is challenging to process and mostly substituted PT derivatives are utilized, for example, poly(3-hexyl thiophene) (P3HT) or PEDOT. Nevertheless, terthiophene was introduced into the MOF pores and polymerized via iodine and heat treatment. The amount of chains formed could be controlled via the monomer feed and the chain conformations were studied via spectroscopic methods as well as molecular dynamics. In contrast to the bulk, a completely  $\pi$ -stacked conformation of the chains was observed, which had an effect on the photophysical properties as well, that is, a blue shift with decreasing monomer loading/number of PT chains per pore.

One of the main features of conjugated polymers is their electrical conductivity, which was investigated by Ballav and coworkers (**Figure 11**).<sup>[128]</sup> Therefore, the MOF based on Cd(2,6-naphthalenedicarboxylate)<sub>0.5</sub>(4-pyridinecarboxylate) was utilized as porous scaffold, loaded with pyrrole monomers and an iodine-mediated polymerization was performed. A substantial increase in conductivity was measured. High carrier density and mobility comparable to inorganic semiconductors was observed via Hall-effect measurements, which was attributed to the interaction of MOF and PPy via  $\pi$ - $\pi$  interactions and N-H- $\pi$  interactions causing percolating conducting pathways through the whole material. Rowe and coworkers utilized HKUST-1 as environment and initiator for PT synthesis.<sup>[129]</sup> On that account, electron-rich oligothiophenes were loaded in the pores of redox active HKUST-1. Under heat, oxidative polymerization was initiated to yield PT inside of the pores. As initiation mechanism a ligand to metal charge transfer followed by a two-electron transfer from oligomers was discussed and indicated by X-ray photoelectron spectroscopy as well as time-dependent density functional theory. Interestingly, substituted EDOT led to oligothiophene coating on the outside of the MOF, which was attributed to the higher electron density of EDOT. Another option is the grafting of conjugated polymers from the MOF surface, for example, via photoinitiated post synthetic modification. Behrens and coworkers studied the grafting from approach of EDOT from a 2D Zr(II)-based MOF.<sup>[130]</sup> As ligand a disubstituted benzophenone derivative was utilized to introduce a photoactive compound that acts as polymerization initiator via ketyl-radical formation after light irradiation. The obtained materials combined the porosity feature of the MOF with the electrical conductivity feature of PEDOT.

In addition to polymerization inside the MOF structure, blending of MOF and polymer is suitable as well to obtain composite materials. It is also a convenient way to produce composite materials on a large scale. For example, Park and coworkers studied the mixture of HKUST-1 and P3HT.<sup>[131]</sup> The composite material was applied as a film on a semiconducting



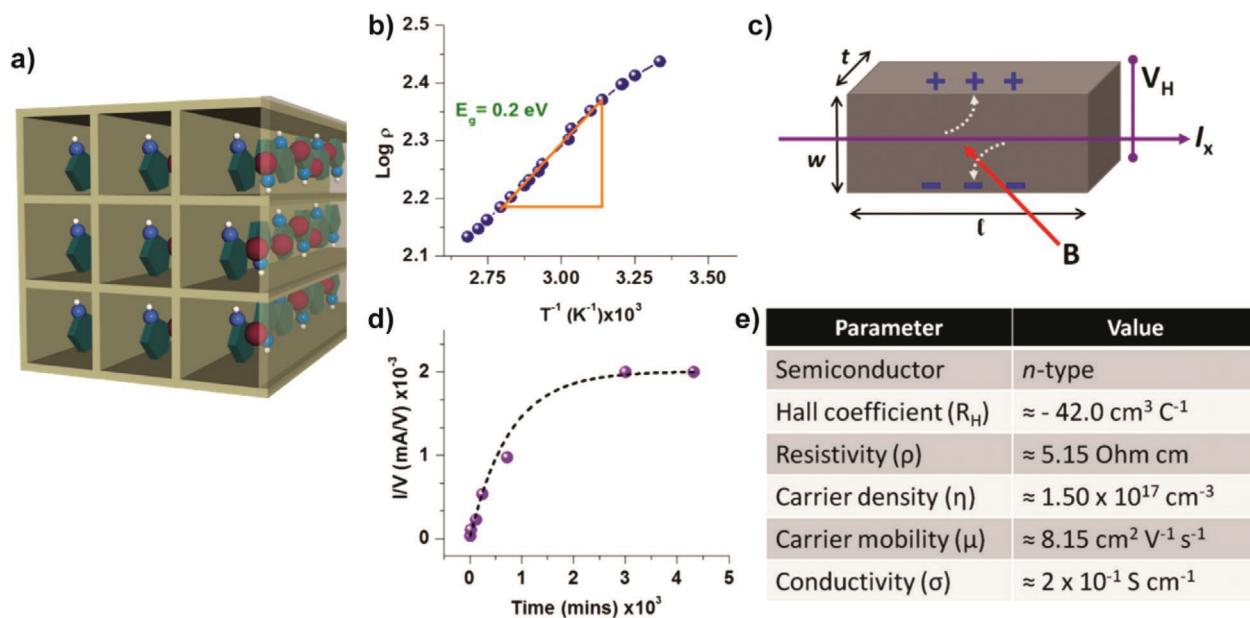


**Figure 11.** a) Schematic of PPy guest incorporation inside MOF host. b) Temperature-dependent electrical conductivity profile of the PPy in MOF system. A linear fit revealed an activation energy  $\approx 0.2 \text{ eV}$  from the slope. c) Schematic diagram of the Hall-effect measurements where  $V_H$ , Hall voltage;  $B$ , magnetic field;  $l$ , length of the sample;  $t$ , thickness of the sample;  $w$ , width;  $I_x$ , current;  $V_H$ ,  $(R_H \cdot I \cdot B / t)$ ;  $R_H$ , Hall coefficient; carrier density ( $\eta$ ) =  $1 / (R_H \cdot e)$ ; Hall mobility ( $\mu$ ) =  $(R_H / \rho)$ ; and  $\rho$ , resistivity. d) Time-dependent  $I$ - $V$  data (from the two-probe method) of PPy in MOF. e) Various parameters obtained from the Hall-effect measurements. Reproduced with permission.<sup>[128]</sup> Copyright 2016, American Chemical Society.

support via spin coating from THF dispersion. The obtained films were utilized as part of organic thin film transistors in order to sense humidity via adsorption of water molecules from the surrounding in the MOF. Ho and coworkers combined sulfonated PT with an MOF based on Zr(II) and meso-tetra(4-carboxyphenyl)porphyrin linkers on carbon cloth in a dye-sensitized solar cell.<sup>[132]</sup> Thus, the composite was deposited on a flexible substrate, where the core carbon was implemented for directed electron transfer and the MOF/polymer coating to trigger the reduction of  $\text{I}_3^-$  via electrocatalysis. A significant electrocatalytic activity was obtained, mainly due to the increased surface area, a good adhesion between carbon cloth and composite coating as well as the formidable electrocatalytic properties of the utilized MOF. As such the obtained cell featured properties close to Pt-based dye-sensitized solar cells.

Being a major trend in polymer materials, 3D printing has found its way into MOF/polymer hybrids and composites as well. Hence, the complexity of MOF-derived materials can be improved even further or new properties introduced into 3D printed scaffolds. For example, Hartings and coworkers described the formation of 3D printed hydrogen storage materials via a combination of acrylonitrile butadiene styrene (ABS) polymer and MOF-5.<sup>[133]</sup> The mechanical properties of the ABS matrix were mainly retained, while significant hydrogen storage capacity was obtained due to the MOF-5 incorporation. In a similar way, Liu and coworkers coated 3D printed ABS with HKUST-1 MOFs via an in situ growth approach.<sup>[134]</sup> Therefore, the 3D printed scaffold was immersed into ligand solution, followed by metal ion solution to form a layer of framework. The process was repeated up to eight times to obtain a layered MOF coating. Finally, the obtained hybrid material was utilized for methylene blue adsorption, which indicates possible

applications in waste water remediation. Rezaei utilized a combination of MOF and PVA to form 3D printed MOF/polymer composites.<sup>[135]</sup> A dispersion of MOF and polymer binder was printed that way. As such, centimeter-sized monoliths could be obtained with decent mechanical properties. Finally, the monoliths were investigated regarding  $\text{CO}_2$  adsorption showing a similar adsorption capacity to the MOF precursor but faster adsorption kinetics. Similarly, Chin and coworkers printed MOF containing polymer scaffolds from a mixture of commercial ink (acrylates, trimethylolpropane propoxylate triacrylate, and EBECRYL 8413) and UiO-66 via photopolymerization.<sup>[136]</sup> In order to introduce porosity, the binder was degraded via thermal treatment leaving an MOF content of 74%. Finally, the MOF monoliths were utilized for catalytic hydrolysis of the pesticide methyl-paraoxon. Magdassi and coworkers dispersed HKUST-1 into a mixture of methacrylate monomer, crosslinker, and photoinitiator.<sup>[137]</sup> Spatially controlled photopolymerization led to the formation of 3D printed scaffolds that could be used to adsorb organic molecules, for example, methylene blue.

In addition to 3D printing, MOFs can be combined with other macroscopic polymer scaffolds to form functional materials as well. Complex responsive material architectures were described by Maspoch and coworkers, who formed 3D structures based on MOF/poly(vinylidene difluoride) (PVDF) films (Figure 12).<sup>[138]</sup> Therefore, MIL-88a MOFs were introduced onto PVDF films with spatial control via an etching process. Due to the adsorption or desorption of humidity, the MIL-88a MOFs could be swollen or shrunken, respectively, which in turn led to a folding of the hybrid film material. Tailored placement of the MOF domains enabled the reversible formation of complex folded 3D architectures or even lifting of small weights. In a similar way, Lang and coworkers fabricated photoresponsive actuators.<sup>[139]</sup>

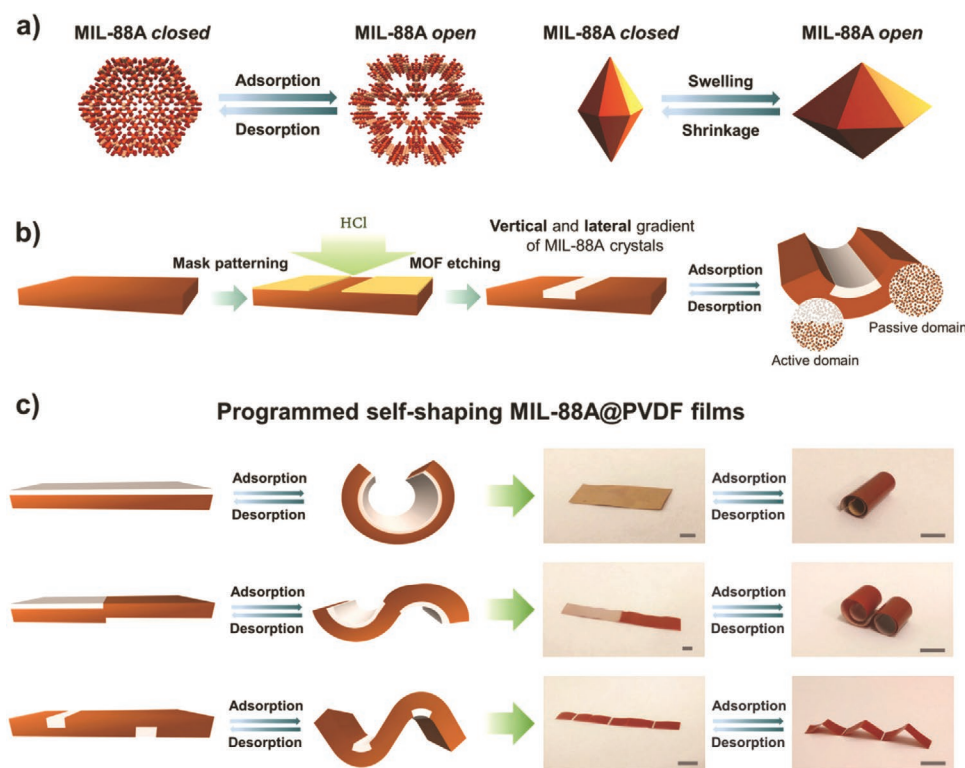


**Figure 12.** a) Scheme of the structural transformation of MIL-88a upon humidity adsorption/desorption (left) and resulting swelling/shrinkage (right). b) Schematic representation of the patterning of MIL-88a/PVDF films by chemical etching with HCl. c) Schematic (left) and photographs (right) of two different patterned MIL-88a/PVDF films, showing multiaxial actuation. (Scale bars = 5 mm). Reproduced with permission.<sup>[138]</sup> Copyright 2019, Wiley-VCH.

To that end, a composite of PVA and a photoreactive MOF, that is, Zn(bdc)(4-(3-fluorostyryl)pyridine), was formed. At first, the PVA film was fabricated and the MOF added to interact with PVA via hydrogen bonding. In the next step the formed composite was subjected to UV light (365 nm), which led to [2 + 2] cycloaddition of the ligands in the MOF and as such to a contraction of the crystal. Accordingly, the overall composite bended due to the contraction of the incorporated material.

A photoresponsive organogel based on metal-organic cages was described by Johnson and coworkers.<sup>[140]</sup> In order to obtain a crosslinked material, homobifunctional PEG with bis-pyridyl dithienylethene endgroups was synthesized that featured two ligand functions to form the metal-organic cages together with metal ions. Moreover, the endgroup was photoresponsive, which reversibly changed the bite angle toward metal-organic cages upon irradiation with UV or green light. Pd(CH<sub>3</sub>CN)<sub>4</sub>(BF<sub>4</sub>)<sub>2</sub> was mixed with the polymeric ligand in acetonitrile to form an organogel. Due to the change in bite angle, different sizes of metal-organic cages were formed, that is, Pd<sub>3</sub>L<sub>6</sub> or Pd<sub>24</sub>L<sub>48</sub>. As such, mechanical properties of the gels could be tuned as well as their self-healing behavior. For example, Pd<sub>3</sub>L<sub>6</sub> featured fast ligand exchange and thus fast self-healing, while Pd<sub>24</sub>L<sub>48</sub> featured slow ligand exchange and no self-healing. Notably, in contrast to organogels, hydrogels containing MOFs were fabricated as well. For example, MOF containing hydrogel monoliths were generated by Liu et al.<sup>[141]</sup> To obtain a hydrogel, ZIF-8, ZIF-67, or UiO-66 were dispersed in a mixture of monomers, that is, acrylamide, HEA, and photoinitiator, in water. The crosslinking

of the hydrogels was enabled by hydrogen bonding between the forming polymer chains and the incorporated MOF crystals. The hydrogels featured significant mechanical properties, for example, tensile strength, compressibility, and durability.

MOF/polymer composite fibers were investigated frequently as well. Zhou and coworkers combined MOFs with cellulose nanofibers via interfacial synthesis for the MOF crystals directly on the fiber surface.<sup>[142]</sup> In a subsequent step, the fibers were converted into free standing nanopapers with high optical transparency, hierarchical porosity, high thermal stability, and high mechanical strength. Finally, the materials were used as filters to remove volatile organic compounds from the air. A fiber hybrid material from MOF and polymer was introduced by Cohen and coworkers, who combined amino functionalized UiO-66 MOF with Nylon.<sup>[143]</sup> Therefore, amino functionalized UiO-66 was grafted with adipoyl chloride in ethyl acetate. In combination with hexamethylenediamine in water, interfacial polymerization was induced that could be used directly to form fibers according to the well-known process of Nylon fiber fabrication. Finally, the fibers were utilized for chemical warfare agent degradation with improved activity compared to physical entrapment or adhesion of the MOF to the fibers.

#### 4.2. MOF/Polymer Membranes

A major topic in polymer/MOF hybrids is the formation of membranes where mixed matrix membranes (MMM) are a very

prominent type.<sup>[144–146]</sup> In such a way, the mechanical properties of polymers can be combined with the defined porosity of MOFs to form durable and selective membranes. Another option is to introduce properties like ion or proton conductivity to the MOF systems via hybridization with polyelectrolytes. The porosity of the MOF system can enhance membrane properties significantly, for example, the flux in separation processes or the selectivity. As such, properties of a polycrystalline MOF membrane can be coupled with the processability and durability of polymer materials. In principle, MOF-polymer membranes can be sorted according to the intended application with gas separation being the most remarkable example.<sup>[147,148]</sup> There are several routes for the fabrication of MOF-based membranes, that is, the in situ growth approach and the adsorption approach. In the case of in situ growth, polymer membranes are combined with metal ions and ligands in cycles in order to grow the MOF directly on top of the polymer phase. The adsorption approach makes use of pre-formed MOF crystallites that are deposited on the polymer scaffold to cover the polymer surface. Moreover, there are several ways to structure MOF/polymer membranes, which has a profound influence on the membrane properties. For example, MOF crystals can be incorporated in a polymer matrix to obtain an MMM.<sup>[149]</sup> Another option is the formation of a thin film of polymer on a pre-formed MOF membrane.<sup>[150]</sup> On the other hand, MOFs can be crystallized on polymer supports as well<sup>[151]</sup> and finally MOF crystals can be mixed with polymer binder to obtain a membrane.<sup>[152]</sup>

In the case of gas separation, a broad variety of examples were described in the literature with binary gas mixtures being the most common, for example, H<sub>2</sub>/CH<sub>4</sub>,<sup>[153]</sup> CO<sub>2</sub>/N<sub>2</sub>,<sup>[150]</sup> H<sub>2</sub>/CO<sub>2</sub>,<sup>[154–157]</sup> or CO<sub>2</sub>/CH<sub>4</sub>.<sup>[158–162]</sup> Moreover, the separation performance of some materials regarding multiple binary gas mixtures was studied as well, for example, H<sub>2</sub>/CH<sub>4</sub> and H<sub>2</sub>/N<sub>2</sub>,<sup>[163]</sup> H<sub>2</sub>/N<sub>2</sub> and H<sub>2</sub>/CH<sub>4</sub> and H<sub>2</sub>/CO<sub>2</sub>,<sup>[164]</sup> CO<sub>2</sub>/CH<sub>4</sub> and CO<sub>2</sub>/N<sub>2</sub>.<sup>[165]</sup> In addition, some studies highlighted the separation behavior of mixtures including the five gases CH<sub>4</sub>, CO<sub>2</sub>, H<sub>2</sub>, N<sub>2</sub>, and O<sub>2</sub>.<sup>[150,166,167]</sup> With respect to gas separation several factors have to be considered, for example, molecular size or polarity of the gas molecules. Gascon and coworkers studied the gas separation of CH<sub>4</sub> and CO<sub>2</sub> (Figure 13).<sup>[158]</sup> At first, MOF nanosheets were synthesized via an interfacial process involving Cu(II) ions in DMF and bdc in benzene. The membrane was formed via dispersion of the MOF nanosheets in a poly(imide) (PI) solution, casted as thin membrane and activated via vacuum. Finally, the membranes were tested regarding gas separation showing significant improvement compared to PI itself and bulk MOF in PI, that is, 30–80% increase in selectivity compared to PI and eightfold increase of selectivity compared to bulk MOF in PI.

A continuous method for the preparation of a polymer on MOF membrane was described by Qiao and coworkers.<sup>[150]</sup> Therefore, NH<sub>2</sub>-MIL-53 MOF was formed on a support material and in a subsequent step an ATRP initiator was attached to the MOF surface via amidation. Finally, polyethylene glycol dimethacrylate was polymerized on the surface to yield a thin polymer film on top of the MOF. The obtained membrane showed significant CO<sub>2</sub> permeability (3000 GPU) and a selectivity of CO<sub>2</sub>/N<sub>2</sub> of 34-fold. Urban and coworkers investigated the pathways of gases to understand the separation in

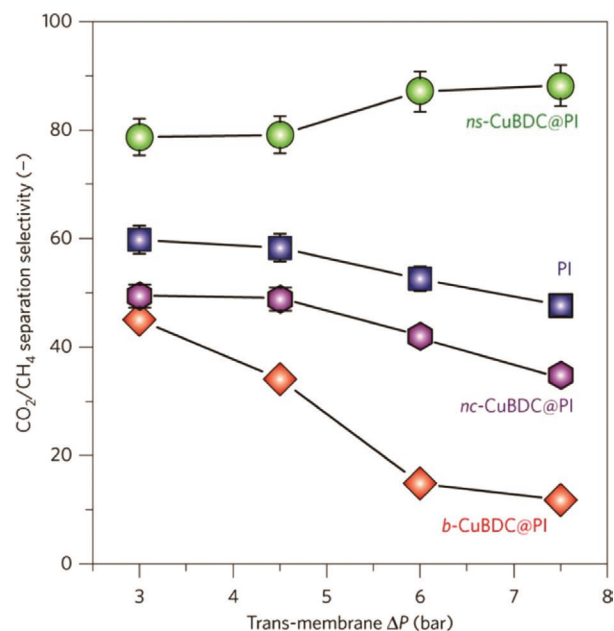


**Figure 13.** Separation selectivity of a MOF-nanosheet (ns)/PI membrane for the permeability of CO<sub>2</sub> and CH<sub>4</sub>, as a function of the pressure difference over the membrane in comparison to a neat PI membrane and other MOF structures (nc, nanoparticle crystals; b, bulk). Reproduced with permission.<sup>[158]</sup> Copyright 2014, Springer Nature.

MOF-based membranes.<sup>[168]</sup> So, a membrane formed from UiO-66-NH<sub>2</sub> was combined with polyethersulfone (PES). High MOF loadings (30–40%) were utilized to introduce dual transport pathways. In such a way, significant CO<sub>2</sub> permeation could be achieved, while the selectivity over CH<sub>4</sub> and N<sub>2</sub> kept a high value of 22 and 25, respectively.

In addition to gas separation, organic compounds can be separated by MOF/polymer membranes as well.<sup>[169–172]</sup> Livingston formed an MMM based on PI ultrafiltration supports and HKUST-1 via direct growth of the MOF on the polymer.<sup>[171]</sup> In contrast to the in situ growth method the precursors were brought into contact via an interfacial process involving two solvents, that is, metal ions were soaked in the membrane in one solvent and ligands were added afterward via another immiscible solvent. Thus, MOF growth was induced at the boundary only. The final membranes could be utilized for rejection of PS and showed improved permeance compared to in situ growth approaches. Long and coworkers described the separation of ethylene over ethane.<sup>[173]</sup> A PI was combined with an MOF from 2,5-dioxido-1,4-benzenedicarboxylate and various metal ions. Ni- and Co-based MOFs showed the best performance with an increase in selectivity of almost twofold. Other metal-ion-based MOFs showed inferior performance probably due to the increased crystallite size. Another reason is the improved interaction of Ni(II) and Co(II) metal sites with the PI compared to Mg(II) or Mn(II), which leads to improved dispersion of crystallites in the polymer matrix. Overall, the smaller size and improved interaction of Ni(II) and Co(II) MOFs prevents interfacial gaps that would lead to non-selective gas transport instead. As a result, improved separation was obtained for Ni(II) and Co(II) MOFs.

A theme of broad interest is the capture of CO<sub>2</sub>, where MOFs being materials with remarkable surface area are certainly a material class that might be useful. Hence, CO<sub>2</sub> adsorption has been in the focus of researchers as well. For example, Sivaniah and coworkers investigated the utilization of MMM for CO<sub>2</sub> capture.<sup>[174]</sup> Therefore, UiO-66 was functionalized with amines and combined with polymers of intrinsic microporosity in a dispersion for membrane formation. The high permeability of the polymer was combined with the adsorption property of the chemically modified MOF, which highlights the favorable combination of MOF and polymer material.

Another important topic is proton conductive membranes as they are utilized in fuel cells.<sup>[175,176]</sup> Guo and coworkers combined super acidic sulfated Zr-MOF-808 with traditional Nafion to improve proton conductivities.<sup>[177]</sup> The super acidic functions retained enough water to run the fuel cell under low humidity conditions. As such an increase in proton conductivity of 23% was observed. Zhu and coworkers formed a composite membrane of Ca(1-(phosphonomethyl) piperidine-3-carboxylic acid)(H<sub>2</sub>O)<sub>2</sub> microrods and poly(vinylpyrrolidone) (PVP).<sup>[178]</sup> In the microrods, protonated amines acted as proton conducting pathways to yield significant proton conductivity at 298 K. Both components added to the performance, as the MOF provides proton conducting sites and the polymer provides water swelling. Ion exchange on the other hand is of significant interest in waste water remediation and has found broad interest as well. Chan and coworkers formed poly(styrene sulfonate) directly in a MIL-101 MOF.<sup>[73]</sup> As such, an ion exchange material was obtained, where the combination of MOF and polymer facilitated increased ion exchange kinetics due to raised surface area and porosity. Moreover, improved capacity and charge selectivity compared to commercial ion exchange resins was observed. In the case of metal ion separation from water, Wang and coworkers crosslinked MOF crystals via a photopolymerization reaction.<sup>[179]</sup> Thus, a UiO/polymer membrane was fabricated that could be used for Cr(IV) separation from water.

### 4.3. MOF Particles and MOFs in the Dispersed State

Polymers are not only synthesized in MOF pores but also attached to the surface of MOFs (Scheme 4).<sup>[180,181]</sup> Hence, several properties can be installed on the MOF material, for example, dispersibility, protection against the environment, or stimuli response. As such grafting of polymers on MOFs is a useful method to stabilize dispersions of the crystalline particles, which is very useful for various applications, for example, in the biomedical field. For example, PEGylation is a frequently used tool to enhance biocompatibility and bioavailability of MOFs.<sup>[182–186]</sup> Another frequently grafted motif are peptides, for example, proteins<sup>[187,188]</sup> or oligopeptides.<sup>[189–191]</sup> Certainly, one has to keep the metal ion component and possible toxic side effects in mind, especially when applications in vivo are intended. In addition, polymers at or around the surface of MOFs might block the pores, which alters adsorption and guest infiltration behavior.

Polymer-grafted MOFs can be fabricated via grafting-from strategies as well as grafting-to pathways, which requires

initiator functionalized MOFs or MOFs with reactive groups, respectively. For example, Matzger and coworkers covered MOF-5 with a layer of IRMOF-3 that was modified with ATRP initiator ligands.<sup>[192]</sup> In a subsequent step, PMMA was grafted from the MOF surface to reveal a shell@shell@core architecture. After hydrolysis of the MOF and release of free polymer, SEC was performed showing high molar masses between 421 and 615 kg mol<sup>-1</sup> and  $\bar{D}$  around 1.3–1.4. Another approach for polymer grafting-from MOFs was introduced by Li and coworkers.<sup>[193]</sup> A copolymer of acrylic acid and an ATRP initiator functionalized monomer was utilized to coat MOF particles, for example, UiO-66, ZIF-8 or MIL-96. Subsequently, polymers were grafted from the coating layer. Various polymer types were grafted to tailor hydrophilicity, dispersibility, or stability against chemicals, for example, PS, PHEA, P4VP, PBMA, or PDMAEMA. In another study, the MOF UiO-66 was grafted with poly(*N*-isopropylacrylamide) (PNIPAM)—a thermoresponsive polymer that changes from the coil state to globule state upon heating in water.<sup>[194]</sup> For the attachment, active ester chemistry was utilized, that is, active ester end functionalized PNIPAM was grafted onto amine functionalized UiO-66. Due to the attachment of globule forming polymer grafts, the MOF surface could be blocked or freed according to temperature. Subsequently, the MOF pores and surfaces were loaded with drug molecules, which could be released at low surrounding temperature due to a permeable polymer shell.

Wuttke and coworkers grafted PEG or an oligoamino amide (Stp10-C) onto the MIL-100 MOF (Figure 14).<sup>[195]</sup> In such a way colloidally stable material was obtained with good cellular uptake and low cytotoxicity. Moreover, fluorescent labels were attached that could be used for fluorescence imaging, while the Fe(III) in the MOF was exploited for magnetic resonance imaging (MRI). Kitagawa and coworkers described a polymer attachment on metal-organic polyhedrons (MOP).<sup>[196]</sup> At first, a grafting-from approach was utilized, MOP were formed from Cu(II) and a RAFT agent containing ligand. A subsequent RAFT polymerization of styrene or *tert*-butyl acrylate led to polymer-grafted MOPs, while the individual polymer arms could be studied after degradation of the MOP. Another option was the utilization of the ligand RAFT agent for polymerization before MOP formation. The polymer product was used in the next step for the self-assembly of an MOP core after Cu(II) addition. In this case, the different polymeric ligands could be used to form miktoarm structures and control the number of arms.

In addition to the grafting approaches, dispersed MOF/polymer hybrids can be formed by other methods as well, for example, the growth of MOFs on polymer particles, the physical attachment of polymers onto MOF particles, or the blending of polymers and MOF particles. Macroscopic polymer beads with integrated MOFs were fabricated by Stylianou and coworkers.<sup>[197]</sup> The beads were fabricated via co-precipitation of HKUST-1 and polymer, for example, PES, poly(etherimide), and PVDF. As such a blend material of MOF and polymer was formed. The obtained millimeter-sized beads were utilized for I<sub>2</sub> capture and recovery from gas streams, for example, in a column setup with the beads as stationary phase. Particle nanostructures formed from MOF and polymer, namely MOF-PDA nanogels, were described by Chen and coworkers.<sup>[198]</sup> Therefore, Mn(II) was complexed with DA and K<sub>3</sub>[Co(CN)<sub>6</sub>] added



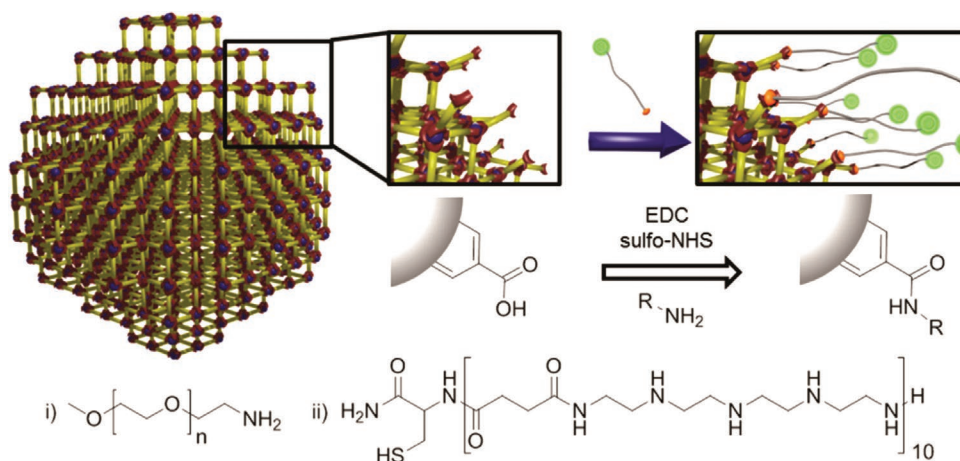


**Figure 14.** Schematic illustration of MOF polymer grafting-to via amidation by 1-ethyl-3-(3-dimethylaminopropyl)carbodiimide hydrochloride and sulfo-NHS mediation. Chemical structures of the grafted polymers: (i) PEG and (ii) Stp10-C. Reproduced with permission.<sup>[195]</sup> Copyright 2016, American Chemical Society.

as linker, which led to MOF formation. DA polymerized inside of the MOF via oxidation to form stable particles. In the next step, the particles were coated for surface tailoring, that is, the particles were PEGylated and cyclic RGD was added for cell targeting. Overall, improved photothermal conversion as well as activity as MRI contrast agent was observed in vivo. Zhang and coworkers formed ZIF-8 particles inside of a poly(acrylic acid) (PAA) template for drug delivery, while the incorporation of PEG-*b*-PAA allowed the formation of PEG functional particles for enhanced biocompatibility.<sup>[199]</sup>

Another structure of interest is the formation of MOF-based capsules, which entail tailored pores due to the MOF incorporation. Bradshaw and coworkers utilized a Pickering emulsion approach to form such a kind of capsule (**Figure 15**).<sup>[31]</sup> Hence, MOF nanoparticles were utilized as Pickering stabilizer for dodecane droplets in water. The oil phase contained

styrene and DVB to fabricate a crosslinked shell of PS. After polymerization the MOF particles were locked in place on the polymer layer forming well-defined microcapsules with MOFs in the wall that could be utilized for dye encapsulation. Polymer particles coated by a MOF was described by Hu and coworkers.<sup>[200]</sup> At first, polymer micelles were synthesized from an amphiphilic ABA block copolymer with PEG A blocks and a diselenide connected poly(urethane) block B and loaded with doxorubicin. In the next step, ZIF-8 MOF particles were grown around the micelle surface. The drug could be released only in acidic (cleavage of the MOF) and reductive environment (cleavage of the diselenides in the block copolymer), while there was no release for the individual triggers. Finally, cytotoxicity, drug release and stability were probed in vitro revealing MOF-polymer micelles as promising platform for drug delivery.

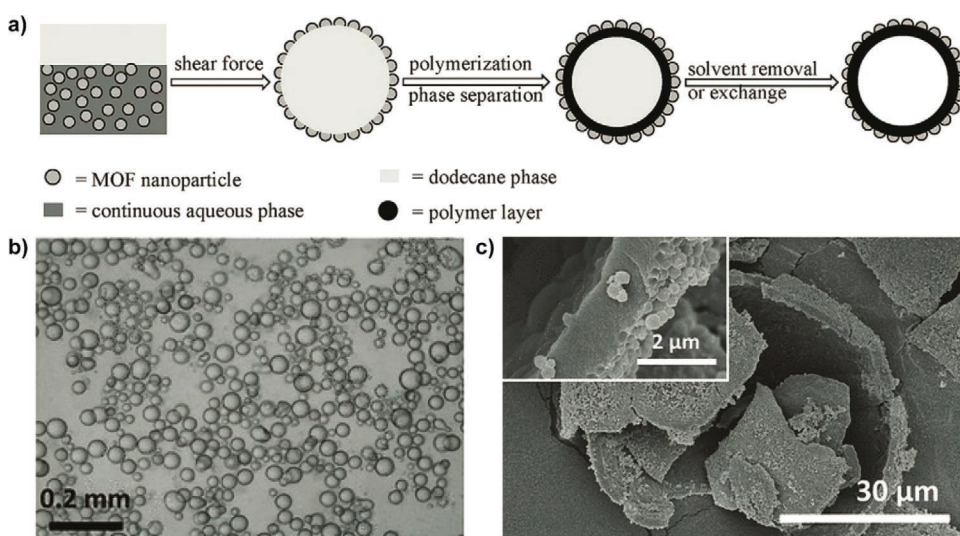


**Figure 15.** a) Schematic overview of MOF-polymer composite capsule formation. b) Optical microscopy image of a typical o/w emulsion stabilized by ZIF-8 nanoparticles. c) SEM image (and inset) of a single broken capsule revealing the hollow interior. Reproduced with permission.<sup>[31]</sup> Copyright 2013, Wiley-VCH.

In a similar way, Richardson and coworkers described the growth of ZIF-8 around poly(saccharides).<sup>[201]</sup> Particle size and morphology could be tailored via the utilized poly(saccharide) template and the concentration. Probably, the hydroxyl groups of the polymers coordinated with Zn(II) in the beginning of the crystallization process for a spatially controlled crystallization. Even cellulose fibers could be covered with MOF crystals to form well-defined core-shell structures. Wong and coworkers described luminescent particle/MOF composites utilizing PVP as binder.<sup>[202]</sup> Therefore, zinc 8-hydroxyquinoline particles were covered with PVP and finally ZIF-8 crystallized around the particles. Notably, the favorable optical properties of the luminescent particle cores were retained.

The inverse structure, namely polymer-coated MOFs, was investigated by Naimi-Jamal and coworkers.<sup>[203]</sup> Therefore, the drug metformin hydrochloride was incorporated into Fe-based MIL-100 and the MOF covered with alginate. The alginate coating led to increased stability and improved control of the drug release process. A coating based on PDA was investigated by Queen and coworkers, who combined HKUST-1 and other MOFs with PDA.<sup>[204]</sup> In a mussel-inspired approach dopamine was polymerized around the respective MOF particles. In a next step 1*H*,1*H*,2*H*,2*H*-perfluorodecanethiol was grafted on the polymer coating to increase the hydrophobicity of the surface. In such a way, the stability of the MOFs against humidity, boiling water, base, and acid increased significantly.

Very recently, Lei and coworkers presented MIL-101 MOF for photodynamic therapy.<sup>[205]</sup> A multilayered MOF was synthesized with black phosphorous quantum dots in the core and the enzyme catalase in the shell. Finally, PEG-folic acid for cell targeting and cyanine labeled caspase substrate peptide for cell apoptosis monitoring were attached to the MOF surface. The catalytic cascade was utilized to convert H<sub>2</sub>O<sub>2</sub> into O<sub>2</sub> and O<sub>2</sub> into <sup>1</sup>O<sub>2</sub>. The encapsulation of the catalytic entities in the MOF led to improved stability in the cell environment and improved <sup>1</sup>O<sub>2</sub> yield for enhanced therapeutic success. Horcajada and coworkers described the coating of MOFs with heparin in order to facilitate drug delivery.<sup>[206]</sup> Overall, improved colloidal stability under physiological conditions was observed, while encapsulation and controlled release features were preserved. In a similar way, Wuttke and coworkers coated Zr-based MOFs with poly(ethylene imine), PAA, PEG, or poly(glutamic acid).<sup>[207]</sup> In particular the coverage with poly(glutamate)-*b*-poly(sarcosine) improved the colloidal stability significantly, for example, in aqueous solutions, protein containing buffer solution, and cellular medium. As such, the system is useful for future applications in the biomedical field. A coating with an alternating copolymer with amphiphilic character was described by del Pino and coworkers.<sup>[208]</sup> Therefore, gold nanostars were covered with ZIF-8 and finally coated with dodecyl-grafted poly(isobutylene-*alt*-maleic anhydride). The amphiphilic polymer protected the MOF from degradation and prevented the drug from release. A near-IR-light-induced release mechanism of a benzamide drug was introduced via coupling of the plasmonic absorption of the core gold nanostars, which created local temperature gradients to trigger thermodiffusion of the drug.

Frequently studied is the combination of MOFs and DNA, which opens up new means of interaction with the environment or amongst the MOF crystals and applications like gene

delivery or biosensing.<sup>[209–211]</sup> For example, Mirkin and coworkers conjugated DNA to UiO-66 MOFs via strain promoted azide-alkyne cycloaddition.<sup>[212]</sup> The conjugation led to improved colloidal stability at increased ion strengths. Next, the cellular uptake of MOF-DNA conjugates was studied with HeLa cells and an improved uptake was found compared to a DNA reference, while cytotoxicity was similar for both reference and conjugate. In a subsequent work, the same team introduced a different way of attachment, that is, via phosphate-mediated interaction.<sup>[213]</sup> Therefore, phosphate-terminated DNA was combined with various MOF types. As such, DNA was conjugated in a versatile and convenient way. Later on, the same method was utilized to fabricate protein delivery vehicles.<sup>[214]</sup> Zr-based MOF nanoparticles were loaded with insulin, conjugated with DNA, and cell internalization studied.

In the realm of biosensors, Li and coworkers described the grafting of single-strand DNA onto UiO-66-NH<sub>2</sub> via amidation and loading of electroactive dyes.<sup>[215]</sup> Finally, a complementary DNA strand was added for partial hybridization with the grafted DNA in order to install a gate keeper for the dyes on the MOF surface. Notably, the added DNA strand was explicitly chosen to be complimentary to the target biomarker. The presence of the respective biomarker-induced hybridization with the gatekeeper DNA strand, which induced release of the electroactive dyes. The detection of the dyes allowed selective sensing of let-7a and miRNA-21 simultaneously. Overall, a selective and sensitive biosensor was obtained. A stimuli-responsive MOF-DNA conjugate was introduced by Willner and coworkers.<sup>[216]</sup> Therefore, cytosine-rich DNA was conjugated to a MOF. Depending on pH the DNA could be switched between coiled structure and *i*-motif, which released or locked the MOF pores, respectively. In addition, another stimulus based on the presence of 18-crown-6-ether/K<sup>+</sup> was investigated as well. In the presence of K<sup>+</sup>, the MOF structure was locked by G-quadruplex formation of the DNA strands that could be released with a return to coil formation via addition of 18-crown-6-ether. Moreover, the MOF was loaded with a dye that could be released via the respective stimulus as well as catalytic activity switched on/off via 18-crown-6-ether/K<sup>+</sup> addition, respectively.

The crystalline structure of MOFs is one of the major aspects of this material class.<sup>[4]</sup> Hence, very defined materials are generated. Although functionalization has been presented before to modify MOF materials, for example, for specific applications,<sup>[5,217]</sup> a rational way to modify the crystals itself would be very beneficial to gain access to a new level of material properties and design. Therefore, the morphology of MOF crystals or MOF particles found significant interest recently.<sup>[218–221]</sup> Inspired by the work of Cölfen and coworkers,<sup>[222,223]</sup> double hydrophilic block copolymer (DHBC)-mediated MOF morphogenesis was studied by our group (Figure 16).<sup>[224]</sup> To that end, poly(methacrylic acid)<sub>8</sub>-*b*-PEG<sub>68</sub> (PMAA<sub>8</sub>-*b*-PEG<sub>68</sub>) was introduced in the MOF synthesis of Zn<sub>2</sub>bdc<sub>2</sub>DABCO that features a tetragonal crystal system and cube-like crystals in the conventional synthesis.<sup>[6]</sup> Nevertheless, addition of PMMA-*b*-PEG to the crystallization yields hexagonal mesocrystals as shown by scanning electron microscopy (SEM) and powder X-ray diffraction, that is, hexagonal rod-like crystals were formed from individual smaller rod-like hexagons in a hierarchical way. The variation of the DHBC DP, that is, PMAA<sub>12</sub>-*b*-PEG<sub>114</sub>, led to another crystal

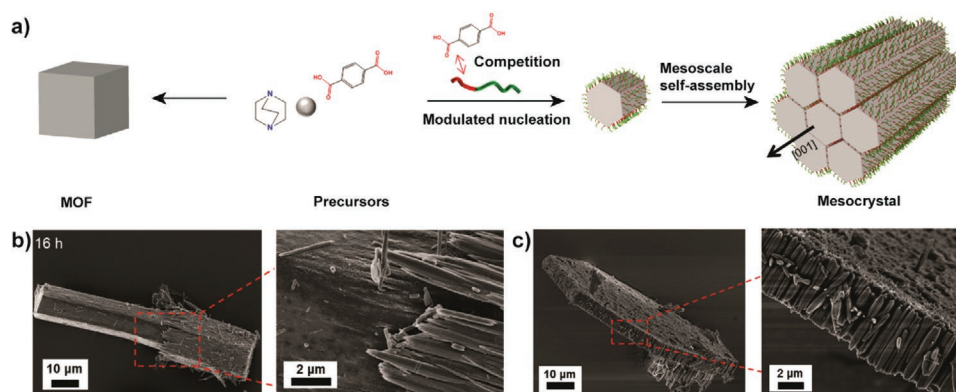


**Figure 16.** a) MOF formation and MOF mesocrystal formation via DHBC mediation. b) SEM images of hexagonal rod-like mesocrystals applying PMAA<sub>8</sub>-*b*-PEG<sub>68</sub>. c) SEM images of hexagonal platelet mesocrystals applying PMAA<sub>12</sub>-*b*-PEG<sub>114</sub>. Reproduced with permission.<sup>[224]</sup> Copyright 2018, American Chemical Society.

morphology namely platelets formed from individual nanorods. As the DP of the PEG block was increased additional steric hindrance disfavors association on top of the nanorods and increased polymer–polymer interactions between the nanorods favors association perpendicular to the rod axis. The formed MOF mesocrystals were covered with DHBC strands on the *bdc*-based side faces of the nanorods. Hence, the large mesocrystals were also covered mainly at the side faces with polymer. Therefore, the DABCO-based top faces remain unoccupied for further association with other MOFs. For example, a combination of plain Zn<sub>2</sub>bdc<sub>2</sub>DABCO with PMAA-*b*-PEG-derived Cu<sub>2</sub>bdc<sub>2</sub>DABCO mesocrystals led to the formation of hybrid MOF materials with spatial control, that is, the mesocrystals associate with DABCO-terminated faces of the Zn<sub>2</sub>bdc<sub>2</sub>DABCO MOF only. As such, ABA (Cu-Zn-Cu) type MOFs were obtained.

Li and coworkers utilized a copolymer to combine different types of MOFs as well.<sup>[225]</sup> The copolymer acted as a mediator for the different mismatched topology and coordination interfaces of the MOFs. At first a core MOF, namely UiO-66, was coated with various copolymers P(MMA-*co*-MAA), P(MMA-*co*-4VP), P(MAA-*co*-4VP), or P(MMA-*co*-MAA-*co*-4VP). Finally, ZIF-8 was grown on the copolymer-coated core MOF, whereas nucleation and growth could be tailored via the utilized copolymer. The MOF on MOF structure could be utilized to perform size selective hydrogenation as the pore size of the outer MOF could be used as size discriminator for the substrate. Notably, the morphology of MOFs can be translated to polymer particles as well as shown by Uemura.<sup>[226]</sup> Accordingly, a polymerization was performed inside of the pores and the MOF template removed via a non-solvent for the polymer. Finally, polymer particles with defined pore structure and shape were formed.

An application of particular interest is the activity of MOFs for catalytic tasks, for example, as mentioned before for polymerization or CuAAC catalysis.<sup>[16,227]</sup> For example, Qiao and coworkers utilized a Cu(II) MOF as catalyst for CuAAC.<sup>[228]</sup> In such a way, small molecules were attached at the end of polymer chains or block copolymers were formed at 150 °C. In a similar way, Duan and coworkers performed CuAAC reactions with a 2D Cu(II) MOF at ambient temperature mediated by visible light.<sup>[229]</sup> While heterogeneous catalysis has several advantages over homogenous catalysis, low dispersibility of

heterogeneous catalysts can have significant influence on catalyst activity.<sup>[230]</sup> To tackle this problem, polymer-MOF hybrids are a promising solution as one of the major drawbacks of most MOF materials is their weak dispersibility that hampers catalyst activity due to decreased accessible surface.<sup>[231,232]</sup> For example, Qian and Webley grafted POEGMA from UiO-66 to increase dispersibility.<sup>[233]</sup> Therefore, ATRP initiators were attached to the MOF surface via esterification and the polymer grafted from the MOF surface. The final MOF particles were well dispersible in water and could be utilized as hydrogenation catalysts after loading with Pd(0) particles. Catalytic activity and recyclability were observed due to the dispersed yet particular nature of the catalyst. Jiang and coworkers studied the catalytic performance of poly(dimethylsiloxane) (PDMS)-coated UiO-66.<sup>[234]</sup> Thus, a composite of UiO-66 and Pd(0) nanoparticles was coated with PDMS to alter the surface wettability. As such, improved catalytic efficiency and recyclability was observed in the hydrogenation of styrene and other reduction reactions. Moreover, the combination of MOF and PDMS prevented nanoparticle aggregation for endured catalytic activity.

Although polymer grafting or coating improves dispersibility, one has to keep in mind that the steric bulk of the polymer around the MOF crystals might hamper the transport of compounds and catalyst activity. Thus, a fine adjustment of the relation between polymer and MOF should be designed in order to optimize activity. The approach of employing a support material,<sup>[235]</sup> for example, the biomaterial pollen,<sup>[236]</sup> seems to be a promising solution to balance accessibility of the crystals with dispersibility and protection from catalyst aggregation. Therefore, a combination of biomaterial-polymer hybrid was investigated as catalyst support by our team (Figure 17).<sup>[237]</sup> Naturally occurring macroporous pollen material was grafted with PDMAEMA via an ATRP grafting-from approach. Hence, the pollen surface was covered with amine containing polymer strands that could associate with Cu<sub>2</sub>bdc<sub>2</sub>DABCO nano-MOF crystals. The final material showed superior dispersibility in organic solvents compared to the MOF itself. Moreover, in comparison to the MOF reference or MOF-polymer aggregates without pollen support an increased catalytic activity for visible-light-triggered CuAAC was observed. This indicates the favorable combination of polymer@pollen support, which can be deduced to an increased dispersibility



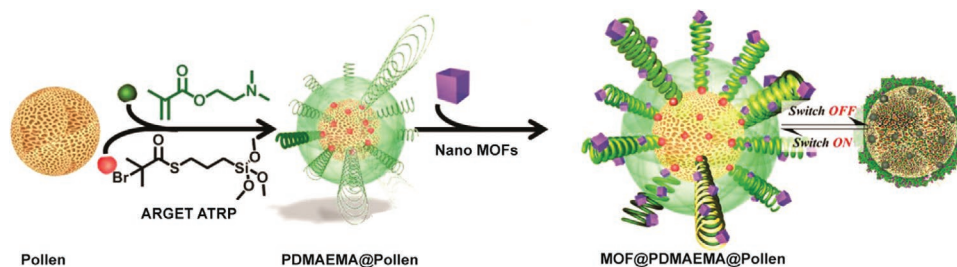


**Figure 17.** Hybrid materials composed of bio-derived pollen grafted with PDMAEMA and MOF association for stimuli-responsive catalysis. Reproduced under the terms of the CC-BY license.<sup>[237]</sup> Copyright 2019, The Authors.

and accessibility of the catalyst due to pollen pivoted polymer grafts. Moreover, the stimulus-responsive aggregation behavior of PDMAEMA could be utilized to switch catalysis “on” or “off” via heating. Another switchable yet pH-responsive catalyst was described by Dong and coworkers.<sup>[238]</sup> Poly(diethylaminoethyl methacrylate) (PDEAEMA) was grafted onto UiO-66 and Pd(0) nanoparticles were formed in the MOF structure via solution impregnation and reduction. The MOF particles were utilized as Pickering stabilizer for toluene in water emulsions. On that account, the MOF particles were used as interfacial catalysts for the Knoevenagel condensation–hydrogenation cascade reaction. Due to the pH-responsive nature of PDEAEMA, emulsions were obtained at neutral conditions and two-phase systems at acidic pH. Finally, the pH-responsive feature could be utilized for easy catalyst separation and recycling.

An approach to combine polymeric catalysts with MOFs was presented by Hatton and coworkers.<sup>[239]</sup> A MIL-101 (Cr) was incorporated into a poly(maleimide-*co*-DVB) network. Bromination of the maleimides led to the formation of *N*-bromomaleimide functions inside of the structure, which featured a similar reactivity to *N*-bromosuccinimide. As such the polymer was introduced to facilitate catalytic tasks, while the MOF particles were introduced for enhanced porosity and surface area. The catalyst materials were utilized for conversion of D-fructose into 5-hydroxymethylfurfural with significant catalytic efficiency and could be readily recycled. A compartmentalization approach of various catalytic polymers inside of an MOF structure was described by Liu and coworkers.<sup>[240]</sup> Therefore, Cr-based MIL-101 was infiltrated with styrene sulfonic acid or a styrenic monomer based on methylaminopyridine. A free radical polymerization was performed to yield two MOF species incorporating two different polymeric catalysts. Finally, both loaded MOFs were combined in one pot to catalyze a cascade reaction, namely deacetalization reaction via acid catalysis followed by a basically catalyzed Knoevenagel reaction. As such two incompatible catalysts could be combined to perform a cascade reaction in one pot, which is not possible without MOF-based compartmentalization.

## 5. Conclusion and Outlook

MOFs and polymers constitute a particularly good combination for the formation of advanced materials. A combination of favorable features of both material types enables the formation of useful materials with unprecedented properties. For example, well-defined pores can be introduced into polymers or improved

processability and materials properties to MOFs. Moreover, MOFs can be utilized to alter polymerization processes and as templates for complex material architectures. As such, MOFs can be employed for polymer synthesis, for example, as catalysts in ATRP or RAFT polymerization. The heterogeneous catalysts feature recyclability, a broad monomer scope, less catalyst contamination in the product and light or thermal activation. In addition, MOFs can be utilized for coordination polymerization acting as well-defined single-site catalysts. In the future, further development regarding MOF polymerization catalysts can be expected. For example, the effect of MOF dispersibility and accessibility of catalytic sites has to be investigated further, which might enable even more sophisticated control of polymerization reactions. As such, targets could be improved tacticity, advanced recycling protocols, or additional external triggers.

Moreover, the well-defined porous structure of MOFs can be used as environment for polymerization reactions for a variety of monomers. Therefore, an improved control over polymer tacticity compared to the bulk as well as otherwise impossible polymer structures can be received. One of the main disadvantages of such approaches is the need for the removal of the MOF template and certainly solutions to those issues will be subject of future research. Nevertheless, the area of polymerization in (MOF) confinement holds several stages of progress that will be tackled in the future, such as enhanced sequence control. The mechanism of polymerization inside of the MOF, especially in the case of RDRP, is still largely unexplored and should gain more attention in the coming years. In particular, improved understanding of such processes might allow conclusions on natural polymerization processes as well.

The combination of MOFs and polymers is not limited to the polymerization process itself. A broad range of literature is available about MOF/polymer hybrid materials with applications ranging from gas adsorption, separation, electrical conductivity, biomedical imaging, drug delivery, to catalysis. As such, the hybridization opens up new opportunities for applications and improvement of existing approaches alike. Moreover, MOFs can be utilized to fabricate specific well-defined polymer architectures and vice versa, which might have a significant impact on properties and applications in the long run. Notwithstanding, structure–property relationships can be deduced and utilized to synthesize materials tailored specifically to the needs of the application. Therefore, one can predict that structural control will be one of the important avenues for researchers in the coming years, addressing new applications as well as improving existing ones. Overall, MOFs and



polymers are a particularly good combination of materials for various directions and promising future developments can be expected without any doubt. Especially in the quest of precisely controlled material structures, the connection between MOF and polymers seems to be a valuable approach.

## Acknowledgements

B.V.K.J.S. acknowledges the Max Planck Society and the University of Glasgow for support.

## Conflict of Interest

The author declares no conflict of interest.

## Keywords

composites, hybrids, metal-organic frameworks, polymers

Received: July 12, 2019

Revised: August 16, 2019

Published online: August 30, 2019

- [1] Y. Zhai, Y. Ma, S. N. David, D. Zhao, R. Lou, G. Tan, R. Yang, X. Yin, *Science* **2017**, 355, 1062.
- [2] A. Baudler, M. Langner, C. Rohr, A. Greiner, U. Schröder, *ChemSusChem* **2017**, 10, 253.
- [3] N. Saba, M. P. Tahir, M. Jawaid, *Polymers* **2014**, 6, 2247.
- [4] H.-C. Zhou, J. R. Long, O. M. Yaghi, *Chem Rev.* **2012**, 112, 673.
- [5] H. Furukawa, K. E. Cordova, M. O'Keeffe, O. M. Yaghi, *Science* **2013**, 341, 1230444.
- [6] D. N. Dybtsev, H. Chun, K. Kim, *Angew. Chem., Int. Ed.* **2004**, 43, 5033.
- [7] S. S. Y. Chui, S. M. F. Lo, J. P. H. Charmant, A. G. Orpen, I. D. Williams, *Science* **1999**, 283, 1148.
- [8] M. Eddaoudi, J. Kim, N. Rosi, D. Vodak, J. Wachter, M. Keffe, O. M. Yaghi, *Science* **2002**, 295, 469.
- [9] T. Loiseau, C. Serre, C. Huguenard, G. Fink, F. Taulelle, M. Henry, T. Bataille, G. Férey, *Chem. - Eur. J.* **2004**, 10, 1373.
- [10] K. Barthelet, J. Marrot, G. Férey, D. Riou, *Chem. Commun.* **2004**, 520.
- [11] C. Serre, C. Mellot-Draznieks, S. Surblé, N. Audebrand, Y. Filinchuk, G. Férey, *Science* **2007**, 315, 1828.
- [12] G. Férey, C. Mellot-Draznieks, C. Serre, F. Millange, J. Dutour, S. Surblé, I. Margiolaki, *Science* **2005**, 309, 2040.
- [13] H. Li, M. Eddaoudi, M. O'Keeffe, O. M. Yaghi, *Nature* **1999**, 402, 276.
- [14] J. H. Cavka, S. Jakobsen, U. Olsbye, N. Guillou, C. Lamberti, S. Bordiga, K. P. Lillerud, *J. Am. Chem. Soc.* **2008**, 130, 13850.
- [15] K. S. Park, Z. Ni, A. P. Côté, J. Y. Choi, R. Huang, F. J. Uribe-Romo, H. K. Chae, M. O'Keeffe, O. M. Yaghi, *Proc. Natl. Acad. Sci. USA* **2006**, 103, 10186.
- [16] J. Lee, O. K. Farha, J. Roberts, K. A. Scheidt, S. T. Nguyen, J. T. Hupp, *Chem. Soc. Rev.* **2009**, 38, 1450.
- [17] B. Li, H.-M. Wen, W. Zhou, B. Chen, *J. Phys. Chem. Lett.* **2014**, 5, 3468.
- [18] M. Lismont, L. Dreesen, S. Wuttke, *Adv. Funct. Mater.* **2017**, 27, 1606314.
- [19] T. Tsuruoka, S. Furukawa, Y. Takashima, K. Yoshida, S. Isoda, S. Kitagawa, *Angew. Chem., Int. Ed.* **2009**, 48, 4739.
- [20] D. Alezi, Y. Belmabkhout, M. Suyetin, P. M. Bhatt, Ł. J. Weseliński, V. Solovyeva, K. Adil, I. Spanopoulos, P. N. Trikalitis, A.-H. Ermas, M. Eddaoudi, *J. Am. Chem. Soc.* **2015**, 137, 13308.
- [21] Y. Li, R. T. Yang, *Langmuir* **2007**, 23, 12937.
- [22] J. Gascon, A. Corma, F. Kapteijn, F. X. Llabres i Xamena, *ACS Catal.* **2014**, 4, 361.
- [23] Q. Fu, K. Xie, S. Tan, J. M. Ren, Q. Zhao, P. A. Webley, G. G. Qiao, *Chem. Commun.* **2016**, 52, 12226.
- [24] S. Yuan, L. Zou, H. Li, Y.-P. Chen, J. Qin, Q. Zhang, W. Lu, M. B. Hall, H.-C. Zhou, *Angew. Chem., Int. Ed.* **2016**, 55, 10776.
- [25] H. L. Nguyen, T. T. Vu, D. Le, T. L. H. Doan, V. Q. Nguyen, N. T. S. Phan, *ACS Catal.* **2017**, 7, 338.
- [26] J. Zhang, F. Dumur, P. Horcajada, C. Livage, P. Xiao, J. P. Fouassier, D. Gigmes, J. Lalevée, *Macromol. Chem. Phys.* **2016**, 217, 2534.
- [27] K. M. Choi, K. Na, G. A. Somorjai, O. M. Yaghi, *J. Am. Chem. Soc.* **2015**, 137, 7810.
- [28] J.-F. Lutz, D. Neugebauer, K. Matyjaszewski, *J. Am. Chem. Soc.* **2003**, 125, 6986.
- [29] J.-F. Lutz, W. Jakubowski, K. Matyjaszewski, *Macromol. Rapid Commun.* **2004**, 25, 486.
- [30] G. Distefano, H. Suzuki, M. Tsujimoto, S. Isoda, S. Bracco, A. Comotti, P. Sozzani, T. Uemura, S. Kitagawa, *Nat. Chem.* **2013**, 5, 335.
- [31] J. Huo, M. Marcello, A. Garai, D. Bradshaw, *Adv. Mater.* **2013**, 25, 2717.
- [32] S. Mochizuki, T. Kitao, T. Uemura, *Chem. Commun.* **2018**, 54, 11843.
- [33] M. Kamigaito, T. Ando, M. Sawamoto, *Chem. Rev.* **2001**, 101, 3689.
- [34] K. Matyjaszewski, J. Xia, *Chem. Rev.* **2001**, 101, 2921.
- [35] H.-C. Lee, M. Antonietti, B. V. K. J. Schmidt, *Polym. Chem.* **2016**, 7, 7199.
- [36] K. Min, H. Gao, K. Matyjaszewski, *Macromolecules* **2007**, 40, 1789.
- [37] J. Wootthikanokkhan, M. Peesan, P. Phinyocheep, *Eur. Polym. J.* **2001**, 37, 2063.
- [38] J. Xia, X. Zhang, K. Matyjaszewski, *Macromolecules* **1999**, 32, 3531.
- [39] W. Jiang, X. Wang, J. Chen, Y. Liu, H. Han, Y. Ding, Q. Li, J. Tang, *ACS Appl. Mater. Interfaces* **2017**, 9, 26948.
- [40] H. L. Nguyen, T. T. Vu, D.-K. Nguyen, C. A. Trickett, T. L. H. Doan, C. S. Diercks, V. Q. Nguyen, K. E. Cordova, *Commun. Chem.* **2018**, 1, 70.
- [41] A. Reyhani, H. Ranji-Burachaloo, T. G. McKenzie, Q. Fu, G. G. Qiao, *Macromolecules* **2019**, 52, 3278.
- [42] Q. Fu, H. Ranji-Burachaloo, M. Liu, T. G. McKenzie, S. Tan, A. Reyhani, M. D. Nothling, D. E. Dunstan, G. G. Qiao, *Polym. Chem.* **2018**, 9, 4448.
- [43] M. A. Tasdelen, M. Ciftci, Y. Yagci, *Macromol. Chem. Phys.* **2012**, 213, 1391.
- [44] F. A. Leibfarth, K. M. Mattson, B. P. Fors, H. A. Collins, C. J. Hawker, *Angew. Chem., Int. Ed.* **2013**, 52, 199.
- [45] D. Konkolewicz, K. Schröder, J. Buback, S. Bernhard, K. Matyjaszewski, *ACS Macro Lett.* **2012**, 1, 1219.
- [46] N. Corrigan, J. Yeow, P. Judzewitsch, J. Xu, C. Boyer, *Angew. Chem., Int. Ed.* **2019**, 58, 5170.
- [47] Y. Liu, D. Chen, X. Li, Z. Yu, Q. Xia, D. Liang, H. Xing, *Green Chem.* **2016**, 18, 1475.
- [48] H. Xing, D. Chen, X. Li, Y. Liu, C. Wang, Z. Su, *RSC Adv.* **2016**, 6, 66444.
- [49] X. Li, D. Chen, Y. Liu, Z. Yu, Q. Xia, H. Xing, W. Sun, *CrystEngComm* **2016**, 18, 3696.
- [50] H.-C. Lee, M. Fantin, M. Antonietti, K. Matyjaszewski, B. V. K. J. Schmidt, *Chem. Mater.* **2017**, 29, 9445.
- [51] H. L. Nguyen, F. Gándara, H. Furukawa, T. L. H. Doan, K. E. Cordova, O. M. Yaghi, *J. Am. Chem. Soc.* **2016**, 138, 4330.



- [52] H. M. Tran, L.-T. T. Nguyen, T. H. Nguyen, H. L. Nguyen, N. T. S. Phan, G. Zhang, T. Yokozawa, H. L. Tran, P. T. Mai, H. T. Nguyen, *Eur. Polym. J.* **2019**, *116*, 190.
- [53] A. Held, F. M. Bauers, S. Mecking, *Chem. Commun.* **2000**, 301.
- [54] R. J. Comito, K. J. Fritzsche, B. J. Sundell, K. Schmidt-Rohr, M. Dincă, *J. Am. Chem. Soc.* **2016**, *138*, 10232.
- [55] R. J. Comito, Z. Wu, G. Zhang, J. A. Lawrence Iii, M. D. Korzyński, J. A. Kehl, J. T. Miller, M. Dincă, *Angew. Chem., Int. Ed.* **2018**, *57*, 8135.
- [56] B. Liu, S. Jie, Z. Bu, B.-G. Li, *J. Mol. Catal. A: Chem.* **2014**, *387*, 63.
- [57] M. Rivera-Torrente, P. D. Pletcher, M. K. Jongkind, N. Nikolopoulos, B. M. Weckhuysen, *ACS Catal.* **2019**, *9*, 3059.
- [58] P. Ji, J. B. Solomon, Z. Lin, A. Johnson, R. F. Jordan, W. Lin, *J. Am. Chem. Soc.* **2017**, *139*, 11325.
- [59] M. J. Vitorino, T. Devic, M. Tromp, G. Férey, M. Visseaux, *Macromol. Chem. Phys.* **2009**, *210*, 1923.
- [60] R. C. Klet, S. Tussupbayev, J. Borycz, J. R. Gallagher, M. M. Stalzer, J. T. Miller, L. Gagliardi, J. T. Hupp, T. J. Marks, C. J. Cramer, M. Delferro, O. K. Farha, *J. Am. Chem. Soc.* **2015**, *137*, 15680.
- [61] R. J. C. Dubey, R. J. Comito, Z. Wu, G. Zhang, A. J. Rieth, C. H. Hendon, J. T. Miller, M. Dincă, *J. Am. Chem. Soc.* **2017**, *139*, 12664.
- [62] C. J. Chuck, M. G. Davidson, M. D. Jones, G. Kociok-Köhn, M. D. Lunn, S. Wu, *Inorg. Chem.* **2006**, *45*, 6595.
- [63] K. Landfester, N. Bechthold, F. Tiarks, M. Antonietti, *Macromolecules* **1999**, *32*, 2679.
- [64] S. Kobayashi, H. Uyama, S. Kimura, *Chem. Rev.* **2001**, *101*, 3793.
- [65] Y. E. Kim, M. S. Hipp, A. Bracher, M. Hayer-Hartl, F. Ulrich Hartl, *Annu. Rev. Biochem.* **2013**, *82*, 323.
- [66] J. Canivet, S. Aguado, C. Daniel, D. Farrusseng, *ChemCatChem* **2011**, *3*, 675.
- [67] M. Lee, S. M. Shin, N. Jeong, P. K. Thallapally, *Dalton Trans.* **2015**, *44*, 9349.
- [68] T. Uemura, N. Yanai, S. Kitagawa, *Chem. Soc. Rev.* **2009**, *38*, 1228.
- [69] T. Uemura, K. Kitagawa, S. Horike, T. Kawamura, S. Kitagawa, M. Mizuno, K. Endo, *Chem. Commun.* **2005**, 5968.
- [70] T. Uemura, Y. Ono, K. Kitagawa, S. Kitagawa, *Macromolecules* **2008**, *41*, 87.
- [71] T. Uemura, Y. Ono, Y. Hijikata, S. Kitagawa, *J. Am. Chem. Soc.* **2010**, *132*, 4917.
- [72] T. Uemura, N. Uchida, A. Asano, A. Saeki, S. Seki, M. Tsujimoto, S. Isoda, S. Kitagawa, *J. Am. Chem. Soc.* **2012**, *134*, 8360.
- [73] L. Gao, C.-Y. V. Li, K.-Y. Chan, *Chem. Mater.* **2015**, *27*, 3601.
- [74] T. Uemura, R. Nakanishi, S. Mochizuki, Y. Murata, S. Kitagawa, *Chem. Commun.* **2015**, *51*, 9892.
- [75] T. Uemura, T. Kaseda, Y. Sasaki, M. Inukai, T. Toriyama, A. Takahara, H. Jinnai, S. Kitagawa, *Nat. Commun.* **2015**, *6*, 7473.
- [76] H.-C. Lee, J. Hwang, U. Schilde, M. Antonietti, K. Matyjaszewski, B. V. K. J. Schmidt, *Chem. Mater.* **2018**, *30*, 2983.
- [77] J. Hwang, H.-C. Lee, M. Antonietti, B. V. K. J. Schmidt, *Polym. Chem.* **2017**, *8*, 6204.
- [78] T. Uemura, D. Hiramatsu, Y. Kubota, M. Takata, S. Kitagawa, *Angew. Chem., Int. Ed.* **2007**, *46*, 4987.
- [79] T. Uemura, R. Nakanishi, T. Kaseda, N. Uchida, S. Kitagawa, *Macromolecules* **2014**, *47*, 7321.
- [80] T. Uemura, N. Uchida, M. Higuchi, S. Kitagawa, *Macromolecules* **2011**, *44*, 2693.
- [81] T. Uemura, S. Mochizuki, S. Kitagawa, *ACS Macro Lett.* **2015**, *4*, 788.
- [82] Y. Kobayashi, K. Honjo, S. Kitagawa, J. Gwyther, I. Manners, T. Uemura, *Chem. Commun.* **2017**, *53*, 6945.
- [83] T. Uemura, R. Kitaura, Y. Ohta, M. Nagaoka, S. Kitagawa, *Angew. Chem., Int. Ed.* **2006**, *45*, 4112.
- [84] Y. Kobayashi, Y. Horie, K. Honjo, T. Uemura, S. Kitagawa, *Chem. Commun.* **2016**, *52*, 5156.
- [85] T. Kitao, M. W. MacLean, B. Le Ouay, Y. Sasaki, M. Tsujimoto, S. Kitagawa, T. Uemura, *Polym. Chem.* **2017**, *8*, 5077.
- [86] T. Kitao, Y. Sasaki, S. Kitagawa, Y. Imamura, M. Tsujimoto, S. Seki, T. Uemura, *J. Phys. Chem. C* **2018**, *122*, 24182.
- [87] R. Haldar, B. Sen, S. Hurre, T. Kitao, R. Sankhla, B. Kühl, A. Welle, S. Heissler, G. Brenner-Weiß, P. Thissen, *Eur. Polym. J.* **2018**, *109*, 162.
- [88] T. Wang, M. Farajollahi, S. Henke, T. Zhu, S. R. Bajpe, S. Sun, J. S. Barnard, J. S. Lee, J. D. W. Madden, A. K. Cheetham, S. K. Smoukov, *Mater. Horiz.* **2017**, *4*, 64.
- [89] C. Lu, T. Ben, S. Xu, S. Qiu, *Angew. Chem., Int. Ed.* **2014**, *53*, 6454.
- [90] Z.-G. Gu, W.-Q. Fu, M. Liu, J. Zhang, *Chem. Commun.* **2017**, *53*, 1470.
- [91] S. Mochizuki, N. Ogiwara, M. Takayanagi, M. Nagaoka, S. Kitagawa, T. Uemura, *Nat. Commun.* **2018**, *9*, 329.
- [92] S. Anan, Y. Mochizuki, K. Kokado, K. Sada, *Angew. Chem., Int. Ed.* **2019**, *58*, 8018.
- [93] R. Medishetty, I.-H. Park, S. S. Lee, J. J. Vittal, *Chem. Commun.* **2016**, *52*, 3989.
- [94] I.-H. Park, R. Medishetty, H.-H. Lee, C. E. Mulijanto, H. S. Quah, S. S. Lee, J. J. Vittal, *Angew. Chem., Int. Ed.* **2015**, *54*, 7313.
- [95] I.-H. Park, A. Chanthapally, Z. Zhang, S. S. Lee, M. J. Zaworotko, J. J. Vittal, *Angew. Chem., Int. Ed.* **2014**, *53*, 414.
- [96] I.-H. Park, A. Chanthapally, H.-H. Lee, H. S. Quah, S. S. Lee, J. J. Vittal, *Chem. Commun.* **2014**, *50*, 3665.
- [97] S.-Y. Yang, X.-L. Deng, R.-F. Jin, P. Naumov, M. K. Panda, R.-B. Huang, L.-S. Zheng, B. K. Teo, *J. Am. Chem. Soc.* **2014**, *136*, 558.
- [98] T. Ishiwata, A. Michibata, K. Kokado, S. Ferlay, M. W. Hosseini, K. Sada, *Chem. Commun.* **2018**, *54*, 1437.
- [99] T. Ishiwata, Y. Furukawa, K. Sugikawa, K. Kokado, K. Sada, *J. Am. Chem. Soc.* **2013**, *135*, 5427.
- [100] L. Feng, X.-L. Lv, T.-H. Yan, H.-C. Zhou, *J. Am. Chem. Soc.* **2019**, *141*, 10342.
- [101] S. Schmitt, S. Diring, P. G. Weidler, S. Begum, S. Heißler, S. Kitagawa, C. Wöll, S. Furukawa, M. Tsotsalas, *Chem. Mater.* **2017**, *29*, 5982.
- [102] C. Zhou, A. Li, D. Wang, E. Pan, X. Chen, M. Jia, H. Song, *Chem. Commun.* **2019**, *55*, 4071.
- [103] Z. Zhang, H. T. H. Nguyen, S. A. Miller, S. M. Cohen, *Angew. Chem., Int. Ed.* **2015**, *54*, 6152.
- [104] Z. Zhang, H. T. H. Nguyen, S. A. Miller, A. M. Ploskonka, J. B. DeCoste, S. M. Cohen, *J. Am. Chem. Soc.* **2016**, *138*, 920.
- [105] S. Ayala, Z. Zhang, S. M. Cohen, *Chem. Commun.* **2017**, *53*, 3058.
- [106] G. E. M. Schukraft, S. Ayala, B. L. Dick, S. M. Cohen, *Chem. Commun.* **2017**, *53*, 10684.
- [107] S. Ayala, K. C. Bentz, S. M. Cohen, *Chem. Sci.* **2019**, *10*, 1746.
- [108] M. J. MacLeod, J. A. Johnson, *Polym. Chem.* **2017**, *8*, 4488.
- [109] T. Kitao, Y. Zhang, S. Kitagawa, B. Wang, T. Uemura, *Chem. Soc. Rev.* **2017**, *46*, 3108.
- [110] K. A. McDonald, J. I. Feldblyum, K. Koh, A. G. Wong-Foy, A. J. Matzger, *Chem. Commun.* **2015**, *51*, 11994.
- [111] Z. Zhang, H. T. H. Nguyen, S. A. Miller, S. M. Cohen, *Angew. Chem., Int. Ed.* **2015**, *54*, 6152.
- [112] R. Semino, J. C. Moreton, N. A. Ramsahye, S. M. Cohen, G. Maurin, *Chem. Sci.* **2018**, *9*, 315.
- [113] T. Uemura, S. Horike, K. Kitagawa, M. Mizuno, K. Endo, S. Bracco, A. Comotti, P. Sozzani, M. Nagaoka, S. Kitagawa, *J. Am. Chem. Soc.* **2008**, *130*, 6781.
- [114] T. Uemura, N. Yanai, S. Watanabe, H. Tanaka, R. Numaguchi, M. T. Miyahara, Y. Ohta, M. Nagaoka, S. Kitagawa, *Nat. Commun.* **2010**, *1*, 83.
- [115] B. Le Ouay, C. Watanabe, S. Mochizuki, M. Takayanagi, M. Nagaoka, T. Kitao, T. Uemura, *Nat. Commun.* **2018**, *9*, 3635.
- [116] T. Iizuka, K. Honjo, T. Uemura, *Chem. Commun.* **2019**, *55*, 691.

- [117] B. Le Ouay, S. Kitagawa, T. Uemura, *J. Am. Chem. Soc.* **2017**, *139*, 7886.
- [118] N.-D. H. Gamage, K. A. McDonald, A. J. Matzger, *Angew. Chem., Int. Ed.* **2016**, *55*, 12099.
- [119] L. D. O'Neill, H. Zhang, D. Bradshaw, *J. Mater. Chem.* **2010**, *20*, 5720.
- [120] M. Mazaj, N. Z. Logar, E. Žagar, S. Kovačič, *J. Mater. Chem. A* **2017**, *5*, 1967.
- [121] C. L. Calvez, M. Zouboulaki, C. Petit, L. Peeva, N. Shirshova, *RSC Adv.* **2016**, *6*, 17314.
- [122] P. Jin, W. Tan, J. Huo, T. Liu, Y. Liang, S. Wang, D. Bradshaw, *J. Mater. Chem. A* **2018**, *6*, 20473.
- [123] L. Chen, X. Ding, J. Huo, S. El Hankari, D. Bradshaw, *J. Mater. Chem.* **2019**, *54*, 370.
- [124] L. Peng, S. Yang, D. T. Sun, M. Asgari, W. L. Queen, *Chem. Commun.* **2018**, *54*, 10602.
- [125] Q. Fu, L. Wen, L. Zhang, X. Chen, D. Pun, A. Ahmed, Y. Yang, H. Zhang, *ACS Appl. Mater. Interfaces* **2017**, *9*, 33979.
- [126] V. J. Pastore, T. R. Cook, J. Rzyayev, *Chem. Mater.* **2018**, *30*, 8639.
- [127] M. W. A. MacLean, T. Kitao, T. Suga, M. Mizuno, S. Seki, T. Uemura, S. Kitagawa, *Angew. Chem., Int. Ed.* **2016**, *55*, 708.
- [128] B. Dhara, S. S. Nagarkar, J. Kumar, V. Kumar, P. K. Jha, S. K. Ghosh, S. Nair, N. Ballav, *J. Phys. Chem. Lett.* **2016**, *7*, 2945.
- [129] N. Marshall, W. James, J. Fulmer, S. Crittenden, A. B. Thompson, P. A. Ward, G. T. Rowe, *Inorg. Chem.* **2019**, *58*, 5561.
- [130] A. Mohmeyer, A. Schaate, B. Hoppe, H. A. Schulze, T. Heinemeyer, P. Behrens, *Chem. Commun.* **2019**, *55*, 3367.
- [131] Y. J. Jang, Y. E. Jung, G. W. Kim, C. Y. Lee, Y. D. Park, *RSC Adv.* **2019**, *9*, 529.
- [132] T.-Y. Chen, Y.-J. Huang, C.-T. Li, C.-W. Kung, R. Vittal, K.-C. Ho, *Nano Energy* **2017**, *32*, 19.
- [133] M. C. Kreider, M. Sefa, J. A. Fedchak, J. Scherschligt, M. Bible, B. Natarajan, N. N. Klimov, A. E. Miller, Z. Ahmed, M. R. Hartings, *Polym. Adv. Technol.* **2018**, *29*, 867.
- [134] Z. Wang, J. Wang, M. Li, K. Sun, C.-J. Liu, *Sci. Rep.* **2015**, *4*, 5939.
- [135] H. Thakkar, S. Eastman, Q. Al-Naddaf, A. A. Rownaghi, F. Rezaei, *ACS Appl. Mater. Interfaces* **2017**, *9*, 35908.
- [136] A. J. Young, R. Guillet-Nicolas, E. S. Marshall, F. Kleitz, A. J. Goodhand, L. B. L. Glanville, M. R. Reithofer, J. M. Chin, *Chem. Commun.* **2019**, *55*, 2190.
- [137] O. Halevi, J. M. R. Tan, P. S. Lee, S. Magdassi, *Adv. Sustainable Syst.* **2018**, *2*, 1700150.
- [138] J. Troyano, A. Carné-Sánchez, D. MasPOCH, *Adv. Mater.* **2019**, *31*, 1808235.
- [139] Y.-X. Shi, W.-H. Zhang, B. F. Abrahams, P. Braunstein, J.-P. Lang, *Angew. Chem., Int. Ed.* **2019**, *0*.
- [140] Y. Gu, E. A. Alt, H. Wang, X. Li, A. P. Willard, J. A. Johnson, *Nature* **2018**, *560*, 65.
- [141] H. Liu, H. Peng, Y. Xin, J. Zhang, *Polym. Chem.* **2019**, *10*, 2263.
- [142] S. Zhou, M. Strømme, C. Xu, *Chem. – Eur. J.* **2019**, *25*, 3515.
- [143] M. Kalaj, M. S. Denny, K. C. Bentz, J. M. Palomba, S. M. Cohen, *Angew. Chem., Int. Ed.* **2019**, *58*, 2336.
- [144] Y. Zhang, X. Feng, S. Yuan, J. Zhou, B. Wang, *Inorg. Chem. Front.* **2016**, *3*, 896.
- [145] R. Lin, B. Villacorta Hernandez, L. Ge, Z. Zhu, *J. Mater. Chem. A* **2018**, *6*, 293.
- [146] T.-S. Chung, L. Y. Jiang, Y. Li, S. Kulprathipanja, *Prog. Polym. Sci.* **2007**, *32*, 483.
- [147] Z. Kang, L. Fan, D. Sun, *J. Mater. Chem. A* **2017**, *5*, 10073.
- [148] E. Adatoz, A. K. Avci, S. Keskin, *Sep. Purif. Technol.* **2015**, *152*, 207.
- [149] S. Kanehashi, G. Q. Chen, C. A. Scholes, B. Ozcelik, C. Hua, L. Ciddor, P. D. Southon, D. M. D'Alessandro, S. E. Kentish, *J. Membr. Sci.* **2015**, *482*, 49.
- [150] K. Xie, Q. Fu, C. Xu, H. Lu, Q. Zhao, R. Curtain, D. Gu, P. A. Webley, G. G. Qiao, *Energy Environ. Sci.* **2018**, *11*, 544.
- [151] E. Barankova, X. Tan, L. F. Villalobos, E. Litwiller, K.-V. Peinemann, *Angew. Chem., Int. Ed.* **2017**, *56*, 2965.
- [152] R. Zhang, S. Ji, N. Wang, L. Wang, G. Zhang, J.-R. Li, *Angew. Chem., Int. Ed.* **2014**, *53*, 9775.
- [153] L. Ge, W. Zhou, A. Du, Z. Zhu, *J. Phys. Chem. C* **2012**, *116*, 13264.
- [154] D. Nagaraju, D. G. Bhagat, R. Banerjee, U. K. Kharul, *J. Mater. Chem. A* **2013**, *1*, 8828.
- [155] J. Hou, P. D. Sutrisna, Y. Zhang, V. Chen, *Angew. Chem., Int. Ed.* **2016**, *55*, 3947.
- [156] L. Zhang, Z. Hu, J. Jiang, *J. Phys. Chem. C* **2012**, *116*, 19268.
- [157] F. Cacho-Bailo, S. Catalán-Aguirre, M. Etxeberria-Benavides, O. Karvan, V. Sebastian, C. Téllez, J. Coronas, *J. Membr. Sci.* **2015**, *476*, 277.
- [158] T. Rodenas, I. Luz, G. Prieto, B. Seoane, H. Miro, A. Corma, F. Kapteijn, F. X. Llabrés i Xamena, J. Gascon, *Nat. Mater.* **2015**, *14*, 48.
- [159] S. Shahid, K. Nijmeijer, *J. Membr. Sci.* **2014**, *470*, 166.
- [160] B. Zornoza, A. Martinez-Joaristi, P. Serra-Crespo, C. Tellez, J. Coronas, J. Gascon, F. Kapteijn, *Chem. Commun.* **2011**, *47*, 9522.
- [161] O. G. Nik, X. Y. Chen, S. Kaliaguine, *J. Membr. Sci.* **2012**, *413–414*, 48.
- [162] A. Sabetghadam, B. Seoane, D. Keskin, N. Duim, T. Rodenas, S. Shahid, S. Sorribas, C. L. Guillouzer, G. Clet, C. Tellez, M. Daturi, J. Coronas, F. Kapteijn, J. Gascon, *Adv. Funct. Mater.* **2016**, *26*, 3154.
- [163] F. Cacho-Bailo, B. Seoane, C. Téllez, J. Coronas, *J. Membr. Sci.* **2014**, *464*, 119.
- [164] T. Ben, C. Lu, C. Pei, S. Xu, S. Qiu, *Chem. – Eur. J.* **2012**, *18*, 10250.
- [165] S. Basu, A. Cano-Odena, I. F. J. Vankelecom, *Sep. Purif. Technol.* **2011**, *81*, 31.
- [166] E. V. Perez, K. J. Balkus, J. P. Ferraris, I. H. Musselman, *J. Membr. Sci.* **2009**, *328*, 165.
- [167] J. Hu, H. Cai, H. Ren, Y. Wei, Z. Xu, H. Liu, Y. Hu, *Ind. Eng. Chem. Res.* **2010**, *49*, 12605.
- [168] N. C. Su, D. T. Sun, C. M. Beavers, D. K. Britt, W. L. Queen, J. J. Urban, *Energy Environ. Sci.* **2016**, *9*, 922.
- [169] X. Li, Y. Liu, J. Wang, J. Gascon, J. Li, B. Van der Bruggen, *Chem. Soc. Rev.* **2017**, *46*, 7124.
- [170] J. Campbell, J. D. S. Burgal, G. Székely, R. P. Davies, D. C. Braddock, A. Livingston, *J. Membr. Sci.* **2016**, *503*, 166.
- [171] J. Campbell, R. P. Davies, D. C. Braddock, A. G. Livingston, *J. Mater. Chem. A* **2015**, *3*, 9668.
- [172] J. Campbell, G. Székely, R. P. Davies, D. C. Braddock, A. G. Livingston, *J. Mater. Chem. A* **2014**, *2*, 9260.
- [173] J. E. Bachman, Z. P. Smith, T. Li, T. Xu, J. R. Long, *Nat. Mater.* **2016**, *15*, 845.
- [174] B. Ghalei, K. Sakurai, Y. Kinoshita, K. Wakimoto, Ali P. Isfahani, Q. Song, K. Doitomi, S. Furukawa, H. Hirao, H. Kusuda, S. Kitagawa, E. Sivaniah, *Nat. Energy* **2017**, *2*, 17086.
- [175] S. J. Peighambaroudost, S. Rowshanzamir, M. Amjadi, *Int. J. Hydrogen Energy* **2010**, *35*, 9349.
- [176] B. Wu, J. Pan, L. Ge, L. Wu, H. Wang, T. Xu, *Sci. Rep.* **2015**, *4*, 4334.
- [177] H. A. Patel, N. Mansor, S. Gadipelli, D. J. L. Brett, Z. Guo, *ACS Appl. Mater. Interfaces* **2016**, *8*, 30687.
- [178] X. Liang, F. Zhang, W. Feng, X. Zou, C. Zhao, H. Na, C. Liu, F. Sun, G. Zhu, *Chem. Sci.* **2013**, *4*, 983.
- [179] Y. Zhang, X. Feng, H. Li, Y. Chen, J. Zhao, S. Wang, L. Wang, B. Wang, *Angew. Chem., Int. Ed.* **2015**, *54*, 4259.
- [180] R. S. Forgan, *Dalton Trans.* **2019**, *48*, 9037.
- [181] I. Abánades Lázaro, S. Haddad, J. M. Rodrigo-Muñoz, C. Orellana-Tavra, V. del Pozo, D. Fairen-Jimenez, R. S. Forgan, *ACS Appl. Mater. Interfaces* **2018**, *10*, 5255.
- [182] P. Horcajada, T. Chalati, C. Serre, B. Gillet, C. Sebrie, T. Baati, J. F. Eubank, D. Heurtaux, P. Clayette, C. Kreuz, J.-S. Chang, Y. K. Hwang, V. Marsaud, P.-N. Bories, L. Cynober, S. Gil, G. Férey, P. Couvreur, R. Gref, *Nat. Mater.* **2010**, *9*, 172.



- [183] I. Abánades Lázaro, S. Haddad, S. Sacca, C. Orellana-Tavra, D. Fairen-Jimenez, R. S. Forgan, *Chem* **2017**, *2*, 561.
- [184] H. Wang, T. Li, J. Li, W. Tong, C. Gao, *Colloids Surf. A* **2019**, *568*, 224.
- [185] M. Benzaqui, R. Semino, F. Carn, S. R. Tavares, N. Menguy, M. Giménez-Marqués, E. Bellido, P. Horcajada, T. Berthelot, A. I. Kuzminova, M. E. Dmitrenko, A. V. Penkova, D. Roizard, C. Serre, G. Maurin, N. Steunou, *ACS Sustainable Chem. Eng.* **2019**, *7*, 6629.
- [186] I. Abánades Lázaro, S. Haddad, J. M. Rodrigo-Muñoz, R. J. Marshall, B. Sastre, V. del Pozo, D. Fairen-Jimenez, R. S. Forgan, *ACS Appl. Mater. Interfaces* **2018**, *10*, 31146.
- [187] S. Jung, Y. Kim, S.-J. Kim, T.-H. Kwon, S. Huh, S. Park, *Chem. Commun.* **2011**, *47*, 2904.
- [188] W.-L. Liu, S.-H. Lo, B. Singco, C.-C. Yang, H.-Y. Huang, C.-H. Lin, *J. Mater. Chem. B* **2013**, *1*, 928.
- [189] H. Hintz, S. Wuttke, *Chem. Commun.* **2014**, *50*, 11472.
- [190] J. Bonnefoy, A. Legrand, E. A. Quadrelli, J. Canivet, D. Farrusseng, *J. Am. Chem. Soc.* **2015**, *137*, 9409.
- [191] L. Zhang, J. Lei, F. Ma, P. Ling, J. Liu, H. Ju, *Chem. Commun.* **2015**, *51*, 10831.
- [192] K. A. McDonald, J. I. Feldblyum, K. Koh, A. G. Wong-Foy, A. J. Matzger, *Chem. Commun.* **2015**, *51*, 11994.
- [193] S. He, H. Wang, C. Zhang, S. Zhang, Y. Yu, Y. Lee, T. Li, *Chem. Sci.* **2019**, *10*, 1816.
- [194] S. Nagata, K. Kokado, K. Sada, *Chem. Commun.* **2015**, *51*, 8614.
- [195] A. Zimpel, T. Preiß, R. Röder, H. Engelke, M. Ingrisch, M. Peller, J. O. Rädler, E. Wagner, T. Bein, U. Lächelt, *Chem. Mater.* **2016**, *28*, 3318.
- [196] N. Hosono, M. Gochomori, R. Matsuda, H. Sato, S. Kitagawa, *J. Am. Chem. Soc.* **2016**, *138*, 6525.
- [197] B. Valizadeh, T. N. Nguyen, B. Smit, K. C. Stylianou, *Adv. Funct. Mater.* **2018**, *28*, 1801596.
- [198] D. Wang, H. Wu, J. Zhou, P. Xu, C. Wang, R. Shi, H. Wang, H. Wang, Z. Guo, Q. Chen, *Adv. Sci.* **2018**, *5*, 1800287.
- [199] L. Yan, X. Chen, Z. Wang, X. Zhang, X. Zhu, M. Zhou, W. Chen, L. Huang, V. A. L. Roy, P. K. N. Yu, G. Zhu, W. Zhang, *ACS Appl. Mater. Interfaces* **2017**, *9*, 32990.
- [200] W. Zhou, L. Wang, F. Li, W. Zhang, W. Huang, F. Huo, H. Xu, *Adv. Funct. Mater.* **2017**, *27*, 1605465.
- [201] K. Liang, R. Wang, M. Boutter, C. M. Doherty, X. Mulet, J. J. Richardson, *Chem. Commun.* **2017**, *53*, 1249.
- [202] Y. Lei, Y. Sun, H. Zhang, L. Liao, S.-T. Lee, W.-Y. Wong, *Chem. Commun.* **2016**, *52*, 12318.
- [203] T. Azizi Vahed, M. R. Naimi-Jamal, L. Panahi, *New J. Chem.* **2018**, *42*, 11137.
- [204] S. Yang, L. Peng, D. T. Sun, M. Asgari, E. Oveisi, O. Trukhina, S. Bulut, A. Jamali, W. L. Queen, *Chem. Sci.* **2019**, *10*, 4542.
- [205] J. Liu, T. Liu, P. Du, L. Zhang, J. Lei, *Angew. Chem., Int. Ed.* **2019**, *58*, 7808.
- [206] E. Bellido, T. Hidalgo, M. V. Lozano, M. Guillevic, R. Simón-Vázquez, M. J. Santander-Ortega, Á. González-Fernández, C. Serre, M. J. Alonso, P. Horcajada, *Adv. Healthcare Mater.* **2015**, *4*, 1246.
- [207] A. Zimpel, N. Al Danaf, B. Steinborn, J. Kuhn, M. Höhn, T. Bauer, P. Hirschle, W. Schrimpf, H. Engelke, E. Wagner, M. Barz, D. C. Lamb, U. Lächelt, S. Wuttke, *ACS Nano* **2019**, *13*, 3884.
- [208] C. Carrillo-Carrión, R. Martínez, M. F. Navarro Poupard, B. Pelaz, E. Polo, A. Arenas-Vivo, A. Olgiaiti, P. Taboada, M. G. Soliman, Ú. Catalán, S. Fernández-Castillejo, R. Solà, W. J. Parak, P. Horcajada, R. A. Alvarez-Puebla, P. del Pino, *Angew. Chem., Int. Ed.* **2019**, *58*, 7078.
- [209] J. Zhuang, A. P. Young, C.-K. Tsung, *Small* **2017**, *13*, 1700880.
- [210] Z. Wang, Y. Fu, Z. Kang, X. Liu, N. Chen, Q. Wang, Y. Tu, L. Wang, S. Song, D. Ling, H. Song, X. Kong, C. Fan, *J. Am. Chem. Soc.* **2017**, *139*, 15784.
- [211] G. Zhang, D. Shan, H. Dong, S. Cosnier, K. A. Al-Ghanim, Z. Ahmad, S. Mahboob, X. Zhang, *Anal. Chem.* **2018**, *90*, 12284.
- [212] W. Morris, W. E. Briley, E. Auyeung, M. D. Cabezas, C. A. Mirkin, *J. Am. Chem. Soc.* **2014**, *136*, 7261.
- [213] S. Wang, C. M. McGuirk, M. B. Ross, S. Wang, P. Chen, H. Xing, Y. Liu, C. A. Mirkin, *J. Am. Chem. Soc.* **2017**, *139*, 9827.
- [214] S. Wang, Y. Chen, S. Wang, P. Li, C. A. Mirkin, O. K. Farha, *J. Am. Chem. Soc.* **2019**, *141*, 2215.
- [215] J. Chang, X. Wang, J. Wang, H. Li, F. Li, *Anal. Chem.* **2019**, *91*, 3604.
- [216] J. S. Kahn, L. Freage, N. Enkin, M. A. A. Garcia, I. Willner, *Adv. Mater.* **2017**, *29*, 1602782.
- [217] S. M. Cohen, *Chem. Rev.* **2012**, *112*, 970.
- [218] Y. Sakata, S. Furukawa, M. Kondo, K. Hirai, N. Horike, Y. Takashima, H. Uehara, N. Louvain, M. Meilikhov, T. Tsuruoka, S. Isoda, W. Kosaka, O. Sakata, S. Kitagawa, *Science* **2013**, *339*, 193.
- [219] S. Furukawa, J. Reboul, S. Diring, K. Sumida, S. Kitagawa, *Chem. Soc. Rev.* **2014**, *43*, 5700.
- [220] J. Hwang, R. Yan, M. Oschatz, B. V. K. J. Schmidt, *J. Mater. Chem. A* **2018**, *6*, 23521.
- [221] J. Hwang, R. Walczak, M. Oschatz, N. V. Tarakina, B. V. K. J. Schmidt, *Small* **2019**, *15*, 1901986.
- [222] H. Cölfen, M. Antonietti, *Angew. Chem., Int. Ed.* **2005**, *44*, 5576.
- [223] M. Jehannin, A. Rao, H. Cölfen, *J. Am. Chem. Soc.* **2019**, *141*, 10120.
- [224] J. Hwang, T. Heil, M. Antonietti, B. V. K. J. Schmidt, *J. Am. Chem. Soc.* **2018**, *140*, 2947.
- [225] F. Wang, H. Wang, T. Li, *Nanoscale* **2019**, *11*, 2121.
- [226] T. Uemura, T. Kaseda, S. Kitagawa, *Chem. Mater.* **2013**, *25*, 3772.
- [227] P. García-García, M. Müller, A. Corma, *Chem. Sci.* **2014**, *5*, 2979.
- [228] Q. Fu, K. Xie, S. Tan, J. M. Ren, Q. Zhao, P. A. Webley, G. G. Qiao, *Chem. Commun.* **2016**, *52*, 12226.
- [229] X. Guo, L. Zeng, Z. Wang, T. Zhang, C. He, C. Duan, *RSC Adv.* **2017**, *7*, 52907.
- [230] N. Mizuno, M. Misono, *Chem. Rev.* **1998**, *98*, 199.
- [231] E. D. Metzger, R. J. Comito, C. H. Hendon, M. Dincă, *J. Am. Chem. Soc.* **2017**, *139*, 757.
- [232] Q. Sun, H. He, W.-Y. Gao, B. Aguila, L. Wojtas, Z. Dai, J. Li, Y.-S. Chen, F.-S. Xiao, S. Ma, *Nat. Commun.* **2016**, *7*, 13300.
- [233] K. Xie, Q. Fu, Y. He, J. Kim, S. J. Goh, E. Nam, G. G. Qiao, P. A. Webley, *Chem. Commun.* **2015**, *51*, 15566.
- [234] G. Huang, Q. Yang, Q. Xu, S.-H. Yu, H.-L. Jiang, *Angew. Chem., Int. Ed.* **2016**, *55*, 7379.
- [235] A. Schätz, O. Reiser, W. J. Stark, *Chem. - Eur. J.* **2010**, *16*, 8950.
- [236] M. G. Potroz, R. C. Mundargi, J. J. Gillissen, E.-L. Tan, S. Meker, J. H. Park, H. Jung, S. Park, D. Cho, S.-I. Bang, N.-J. Cho, *Adv. Funct. Mater.* **2017**, *27*, 1700270.
- [237] H.-C. Lee, T. Heil, J.-K. Sun, B. V. K. J. Schmidt, *Mater. Horiz.* **2019**, *6*, 802.
- [238] W.-L. Jiang, Q.-J. Fu, B.-J. Yao, L.-G. Ding, C.-X. Liu, Y.-B. Dong, *ACS Appl. Mater. Interfaces* **2017**, *9*, 36438.
- [239] L. Bromberg, X. Su, T. A. Hatton, *Chem. Mater.* **2014**, *26*, 6257.
- [240] J.-H. Zhao, Y. Yang, J.-X. Che, J. Zuo, X.-H. Li, Y.-Z. Hu, X.-W. Dong, L. Gao, X.-Y. Liu **2018**, *24*, 9903.